NACA

RESEARCH MEMORANDUM

ALTITUDE-WIND-TUNNEL INVESTIGATION OF SEVERAL AFTERBURNER CONFIGURATIONS HAVING MODERATELY HIGH BURNER-INLET VELOCITIES

By F. W. Schulze, H. E. Bloomer, and R. R. Miller

Lewis Flight Propulsion Laboratory
Cleveland, Ohio

NATIONAL ADVISORY COMMITTEE
FOR AERONAUTICS

WASHINGTON

November 17, 1954

NATIONAL ADVISORY COMMITTEE FOR AERONAUTICS

RESEARCH MEMORANDUM

ALTITUDE-WIND-TUNNEL INVESTIGATION OF SEVERAL AFTERBURNER CONFIGURATIONS HAVING MODERATELY HIGH BURNER-INLET VELOCITIES

By F. W. Schulze, H. E. Bloomer,
and R. R. Miller

SUMMARY

An altitude investigation of several afterburner configurations having moderately high burner-inlet velocities was conducted in the NACA Lewis altitude wind tunnel. The combustion efficiency and thrust characteristics of several afterburner configurations were determined. The results showed that the presence of whirl angles as great as 30° at the afterburner inlet was detrimental to efficient combustion. Reduction of whirl to less than 10° resulted in increases in combustion efficiency of about 5 percent. These increases in combustion efficiency did not produce reductions in fuel consumption because the pressure losses introduced by the whirl straightening vanes compensated for the gains in combustion efficiency.

INTRODUCTION

An investigation of the altitude performance and operational characteristics of a 36-inch-diameter afterburner on a turbojet engine was conducted in the NACA Lewis altitude wind tunnel. The primary purpose of this investigation was to study the effects of the afterburner internal geometry on screeching combustion. A secondary purpose was to determine the over-all performance of several of these afterburner configurations.

The screech investigation, reported in reference 1, included a large number of afterburner configurations. Several of these configurations are presented herein to show the effects of afterburner-inlet gas whirl pattern, flame-holder design, and fuel distribution on performance as determined by combustion efficiency, augmented thrust ratio, and specific fuel consumption.

Data were obtained over a range of afterburner fuel-air ratios at an average turbine-outlet temperature of 1690° R and turbine-outlet total pressures ranging from 4210 to 760 pounds per square foot absolute. These pressures corresponded to a range of flight Mach numbers from 0.14 to 1.00 at altitudes between 10,000 and 45,000 feet.

APPARATUS

Turbojet Engine

The axial-flow turbojet engine used in the investigation had a sea-level air flow of about 167 pounds per second at the rated engine speed of 6100 rpm. Major engine components included a 16-stage axial-flow compressor, a can-annular-type combustor, and a three-stage turbine. The rated turbine-outlet temperature for afterburning conditions, as indicated by the manufacturer's control thermocouples, was 1670° R. This temperature corresponded to an average temperature of 1690° R as determined by a more comprehensive survey with NACA rakes.

Afterburner Components

A sketch of afterburner configurations 1 and 2, which were patterned from an afterburner used in reference 2, is shown in figure 1. The flame holder, having two annular V-gutters $1\frac{5}{8}$ and $1\frac{7}{8}$ inches in width, blocked 32 percent of the flow area at the flame-holder location $25\frac{3}{16}$ inches downstream of the turbine outlet. The fuel bars could be positioned either $11\frac{5}{8}$ or $17\frac{5}{8}$ inches downstream of the turbine outlet to produce either configurations 1 or 2, respectively. The diffuser inner body, 32 inches in length, terminated in a hemispherical dome. Over-all length of the diffuser, afterburner shell, and iris-type nozzle was $101\frac{1}{2}$ inches. The maximum exhaust-nozzle area was 4.13 square feet. Although not shown, an external air-cooling passage surrounded the aft end of the afterburner and nozzle. The diffuser outer wall and afterburner shell shown in figure 1 were common to all configurations except for changes in the exhaust-nozzle-outlet area and a 6-inch extension of the afterburner length made in the middle of the program.

The alterations to the diffuser, the flame holders, and the fuel systems investigated are described in the following paragraphs. Descriptions of the configurations using these components and the significance of the modifications are given in the RESULTS AND DISCUSSION section, while a listing of the components combined to form a single configuration is given in table I for each of the eight configurations.

Alterations to the diffuser are shown in figure 2. Details of the pilot-type step added to the original inner body to produce a flame seat are shown in figure 2(a). Another modification extended the inner body to form a smooth cone, as shown in figure 2(b). A sketch giving details of the twin-deflector cascade installed in the diffuser passage with the original inner body is shown in figure 2(c), and a photograph of the deflectors installed is shown in figure 2(d). In order to reduce the whirl of the gases leaving the turbine, 48 equally spaced full-passage-width antiwhirl vanes were installed at the inlet to the diffuser. Details of the vanes are given in figure 2(e), and a photograph of the installed vanes is shown in figure 2(f). These vanes, designed with constant camber and varying chord to obtain proper turning angles at all radii, were incorporated into the original inner-body configuration as well as the long extended inner cone.

The four flame holders used in the various configurations are shown in figure 3. Flame holder A was the original flame holder, and flame holders B and C were modifications of the original. These modifications resulted in a gutter width of $2\frac{1}{8}$ inches for flame holder B and a gutter width of $2\frac{1}{4}$ inches for flame holder C. The axial stagger in flame holder C was $3\frac{3}{4}$ inches as compared with $1\frac{1}{4}$ inches for flame holder A, and the trailing edges of the gutters were made nonplanar. Flame holder D comprised four annular V-type gutters having widths of $1\frac{1}{4}$ inches. As shown in figure 3(e), four flame-holder positions were used ranging from $25\frac{3}{16}$ to $42\frac{1}{2}$ inches downstream of the diffuser inlet.

The details of the fuel-spray bars used in the investigation are presented in figure 4. Twenty fuel bars equally spaced around the circumference were used in all instances. The fuel-spray bars designated A (the original), D, E, and F were radial bars each with 10 to 14 orifices providing a spray normal to the flow of gas (side spray) (fig. 4(a)). Fuel bars A and F were identical except for the number of orifices, while bars D and E were identical except for the orifice sizes. Inasmuch as the bars could be located in any one of four positions, the fuel pattern at the flame holder obtained with a given bar was affected by its location. As an aid in visualizing the fuel pattern, the location of the orifices is presented as a percentage of passage height. The size of the orifices varied from 0.0225 to 0.0310 inch in diameter. Fuel bars B and C were denoted as slant bars because the fuel near the inner body was injected farther downstream than the fuel near the outer wall (fig. 4(b)). The slant bars provided side sprays from either 14 or 16 orifices. In one of the configurations, two sets of bars were installed and fuel to each set could be individually controlled and measured.

Instrumentation

A cross section of the engine and the afterburner showing station locations and a tabulation of instrumentation at each station are given in figure 5. Pressure measurements at a 26-inch-diameter venturi in the inlet duct and the temperatures from the rakes at the compressor inlet were used to determine engine air flow. Turbine-outlet or diffuser-inlet conditions were obtained from three rakes located 3 inches downstream of the diffuser inlet. The angle of gas whirl across the passage was measured by a null-type total-pressure yaw probe at a location $5\frac{1}{2}$ inches downstream of the diffuser inlet.

Diffuser-outlet conditions were determined at a station 20 inches downstream of the diffuser inlet by means of two rakes. A 12-tube total-pressure rake and two wall static taps were also used at the 20-inch station and for certain configurations at a station $32\frac{7}{8}$ inches from the diffuser inlet to determine the velocity pattern. The exhaust-nozzle conditions were surveyed 15 inches upstream of the nozzle exit by a vertical water-cooled rake.

The tunnel balance system was used to measure the thrust of the engine and afterburner combination. Instrumentation used to detect and measure screech characteristics is described in reference 1. The symbols and methods of calculation used in this report are presented in appendixes A and B, respectively.

Installation

The engine with the afterburner was mounted on a wing section that spanned the 20-foot-diameter test section of the altitude wind tunnel as shown in figure 6. Dry air was supplied to the engine from the tunnel make-up air system through a duct connected directly to the engine inlet. Engine thrust and installation drag measurements by the tunnel balance system were made possible by use of a slip joint in the inlet-air duct upstream of the engine.

PROCEDURE

The performance characteristics of the afterburner configurations were obtained over a range of afterburner fuel-air ratios at the following simulated flight conditions and diffuser-inlet total pressures:

Altitude, ft	Flight Mach number	Average engine-inlet temperature, °R	Average diffuser-inlet total pressure, lb/sq ft abs
10,000	0.49	516	4210
35,000	1.00	474	2370
35,000	.14	458	1250
45,000	.15	454	760

The flight Mach number is based on complete ram-pressure recovery at the compressor inlet. Engine-inlet temperatures corresponding to NACA standard altitude conditions could not be maintained at all simulated flight conditions. The engine was operated at rated speed and at an indicated turbine-outlet control temperature of 1670° R. Afterburner ignition was accomplished by use of the "hot-streak" method whereby an additional quantity of fuel was injected locally for a short time at the turbine inlet. Afterburner performance data were obtained over a range of fuel-air ratios between either lean blow-out or smallest exhaust-nozzle area and either rich blow-out or maximum nozzle area giving limiting turbine-outlet temperature. The exhaust-nozzle area was manually controlled.

Atmospheric air, throttled to give approximately 3 percent of engine air flow, was used to cool the afterburner shell and iris-nozzle segments. When two sets of fuel bars were used in a configuration, the flow to each set was measured by displacement-type flow meters, while the total flow was measured by calibrated rotameters. Fuel for both the engine and afterburner conformed to MIL-F5624A grade JP-4 specifications.

RESULTS AND DISCUSSION

Afterburner-Inlet Flow Conditions

The velocity distributions and the whirl patterns in the afterburner diffuser were measured at several stations. The velocity patterns, determined by use of the full-passage rakes at stations 3, 20, and $32\frac{7}{8}$ inches downstream of the diffuser inlet, are presented in figures 7(a) and (b). The two downstream stations correspond to diffuser area ratios of 1.70 and 1.95 (ratio of complete diffusion is 2.07). The velocity profile at the 3-inch station is an average of 3 rakes, whereas only a single rake was used in determining the other patterns. As shown in figure 7(a) for an altitude of 35,000 feet and a flight Mach number of 1.00, the average diffuser-inlet velocity was about 900 feet per second. At the $32\frac{7}{8}$-inch station (near the diffuser outlet), the velocity varied from 130 feet per second at 2 percent passage height to 580 feet

per second at 90 percent passage height. As shown in figure 7(b) for an altitude of 45,000 feet and a flight Mach number of 0.15, the average diffuser-inlet velocity was about 1000 feet per second. At the $32\frac{7}{8}$-inch station, the velocity varied from 310 feet per second at 2 percent passage height to 610 feet per second at 80 percent passage height. Although not shown, the velocity profiles at the other flight conditions were similar in magnitude and shape to those presented in figure 7(a). At the initial flame-holder position ($25\frac{3}{16}$ in. downstream of the diffuser inlet), the average velocity is then about 490 feet per second, which is considerably higher than the average for most production afterburners (about 400 ft/sec).

Results of surveys of whirl angle made $5\frac{1}{2}$ inches downstream of the diffuser inlet are presented in figure 7(c). The flow leaving the turbine had a positive or counterclockwise (looking upstream) whirl of 20° to 30° from the axial direction over the inner 70 percent of the passage. Beyond this area, the whirl decreased to a value of about -20° at the outer wall. This large whirl contributed to flow separation, which resulted in low velocities near the inner body, as shown in figures 7(a) and (b). There was no effect of diffuser-inlet pressure on the whirl profile. The diffuser-inlet (afterburner-outlet) temperature during these runs was slightly lower than rated temperature conditions. As shown in figure 7(c), however, the effect of temperature over the range from 1399° to 1634° R is negligible. The single profile presented was believed to apply also at rated conditions.

Performance of Configurations with Initial Whirl Pattern

Description. - The afterburner configurations having the initial flame holder, diffuser, and fuel-spray bars (configurations 1 and 2) differ only in the position of fuel-spray bar A, as can be seen in figure 1. Schematic sketches of configurations 3, 4, 5, which incorporated internal changes to the initial configurations and were tested with the existing severe whirl pattern, are given in figure 8. Only the locations of the fuel bars and the flame holder with respect to the diffuser-exit flange are given inasmuch as other details of the components have been shown in figures 2 to 4. Configuration 3 incorporated the following: (1) a pilot-type step on the inner cone for providing a flame seat, (2) slanting fuel bars B to reduce the fuel mixing length near the inner body and to produce a piloting action in the center region of the burner, and (3) flame holder A moved $6\frac{9}{16}$ inches downstream of the original position.

Because a uniform velocity profile is shown to be desirable in reference 3, annular deflectors to redistribute the mass flow were used in configuration 4 along with flame holder A and slant fuel-spray bars

C altered to inject more fuel near the inner body. The effect of the deflectors on the velocity profile 20 inches downstream of the diffuser inlet is shown for two altitude conditions in figure 9. Gas had been forced radially inward, thereby substantially raising the velocities near the inner cone. The wake from the outer deflector produced a low local velocity at about 60 percent passage height.

Configuration 5 consisted of the modified flame holder B located $17\frac{5}{16}$ inches downstream of the original position, an extended inner cone, and the original radial fuel-spray bars. It was felt that moving the flame holder downstream placed it in a region of lower average velocity (about 430 ft/sec) as well as provided a long fuel mixing length of $27\frac{7}{8}$ inches. Configuration 5 also included an enlarged exhaust nozzle (maximum nozzle area, 4.63 sq ft) and a 6-inch extension of the burner shell.

Performance. - The performance of configurations 1 and 2 is presented for all altitude conditions in figures 10 to 13, while the performance of configurations 3, 4, and 5 at an altitude of 35,000 feet and a flight Mach number of 1.00 is presented in figures 14 and 15.

The diffuser total-pressure losses for configurations 1 and 2 (fig. 10) were between 0.017 and 0.030 of the diffuser-inlet total pressure, with the highest loss occurring at an altitude of 45,000 feet. The over-all total-pressure loss varied from 0.067 to 0.096 at all altitudes except at 45,000 feet, where a loss as high as 0.117 occurred. These higher losses at 45,000 feet were caused by the higher diffuser-inlet velocities.

The combustion efficiencies of configurations 1 and 2 are shown in figure 11. As the afterburner pressure level decreased, the combustion efficiency decreased. A maximum combustion efficiency of 0.87 was reached with both configurations 1 and 2 at a fuel-air ratio of about 0.035 at an altitude of 10,000 feet, where the diffuser-inlet total pressure was 4210 pounds per square foot absolute. Configuration 1 gave 0.02 to 0.03 higher combustion efficiency at all other diffuser-inlet total pressures down to 1250 pounds per square foot absolute. At 760 pounds per square foot absolute, however, combustion could not be obtained with configuration 1. Burning in configuration 2 was possible at this pressure level. The superior altitude limit was most likely caused by the stratification of fuel in this combustor. At a fuel-air ratio of 0.028, efficiency of configuration 2 at the diffuser-inlet pressure level of 760 pounds per square foot absolute was about 0.7. The maximum exhaust-nozzle area limited the maximum fuel-air ratio at all altitudes except at 10,000 feet, where fuel flow was temporarily limited by the facility fuel system. The nozzle area limit was particularly apparent at the 45,000-foot altitude, where performance was obtainable only at fuel-air ratios below 0.032.

Augmented net-thrust ratio, based on the thrust of the engine without an afterburner, reached a maximum value of 1.71 at an altitude of 35,000 feet and a flight Mach number of 1.00 (fig. 12(b)). At the 1.71 augmented net-thrust ratio, specific fuel consumption was 2.03 pounds of fuel per hour per pound of thrust (fig. 13(b)).

The performance of configurations 3, 4, and 5, although obtained at several altitudes, can only be compared at an altitude of 35,000 feet and a flight Mach number of 1.00. These configurations differ from each other by more than one variable, and hence the comparisons illustrate only the relative over-all performance of configurations of different design. Total-pressure losses and combustion efficiencies at this altitude are shown in figures 14(a) and (b), respectively. Pressure-loss characteristics were similar to those of configuration 1, indicating no adverse effect of deflectors or increased flame-holder blockage. Only configuration 3 attained a combustion efficiency slightly higher than the original, and this occurred above a fuel-air ratio of 0.037. However, this configuration with a pilot-type step on the inner body would operate only at burner pressures above about 820 pounds per square foot absolute. Operation at a pressure level of 760 pounds per square foot absolute with the configuration having the deflectors (configuration 4) required that ignition be accomplished at a higher pressure. Combustion screech was encountered at an altitude of 10,000 feet with the configuration having the long fuel-mixing length (configuration 5). A comparison of the augmented thrust ratio and the specific fuel consumption of configurations 3, 4, and 5 with configuration 1 in figures 14(c) and (d), respectively, indicates the general superiority of configuration 1.

Reduction of Whirl

In an initial attempt to reduce whirl, 33 short ($2\frac{1}{2}$-inch span) vanes were attached to the inner cone at the diffuser inlet. However, these proved ineffective, and consequently a set of 48 full-passage vanes were installed (see figs. 2(e) and (f)). The afterburner-inlet flow conditions with the vanes installed are presented in figure 15. For operation at an altitude of 35,000 feet and a flight Mach number of 1.00, the velocity profile $32\frac{7}{8}$ inches downstream of the diffuser inlet (fig. 15(b)) varied from 300 feet per second at 2 percent of the passage height to a peak of 590 feet per second at 52 percent of the passage height. Comparison of this profile with the profile obtained without vanes (dashed line) showed that the peak velocity was about the same and that a redistribution of flow occurred at the expense of raising the average velocity about 40 feet per second.

As shown by the whirl pattern presented in figure 15(c), a substantial improvement over the original pattern occurred when the vanes were installed. The whirl angle was less than 10° over the entire passage.

Performance of Configurations Tested with Reduced Whirl

Description. - Sketches of configurations 6, 7, and 8, which incorporated the antiwhirl vanes and the larger exhaust nozzle, are shown in figure 16. Configuration 6 included the long extended inner cone, flame holder C located in a downstream position, and radial fuel bar D giving $15\frac{1}{4}$ inches of fuel mixing length.

Configuration 7 was almost identical with configuration 6 except for the addition of fuel-spray bar A in position 2, substitution of fuel spray bar E for D, and the use of flame holder D in the downstream position. The four annular V-type gutters of flame-holder D were intended to provide a better distribution of flame stabilization seats. Fuel was injected simultaneously through both sets of spray bars with about 83 percent of total fuel flow injected through the upstream bars.

Configuration 8 combined the original inner body, the flame holder used in configuration 5 at the initial flame-holder position, and fuel bar F at the number 1 position. Blockage of flame holder B in this position was 39 percent of the annular flow area. Fuel bar F is the original fuel bar (A) with 2 orifices added near the diffuser outer wall.

Performance. - Performance of configurations 6, 7, and 8 is presented in figures 17, 18, and 19. Combustion efficiency at the three altitude conditions is shown in figure 17. A maximum combustion efficiency of 0.92 was obtained with the 4-V-gutter flame holder (configuration 7) at a fuel-air ratio of 0.039 and a diffuser-inlet total pressure of 4210 pounds per square foot absolute. The efficiency of this configuration decreased to 0.80 at a pressure level of 2370 pounds per square foot absolute at a fuel-air ratio of 0.038. The 4-V-gutter flame holder, however, would not support combustion at a diffuser-inlet pressure of 760 pounds per square foot absolute, indicating, as in reference 4, that small gutter widths tend to reduce combustion stability limits at low burner-inlet pressures. The 2-V-gutter flame holder with $2\frac{1}{4}$-inch gutter widths was operable at this high altitude, where a combustion efficiency of 0.80 was achieved at a fuel-air ratio of 0.03. However, this value cannot compare with other data because the burner-inlet temperature was inadvertently set at 1800° R. This temperature, which is 110° R higher than average, would be expected to have a marked beneficial effect on combustion. Combustion screech was encountered with this 2-V-gutter flame holder below fuel-air ratios of 0.025 at a pressure of 4210 pounds per square foot absolute. At this same burner pressure level, configuration 8 produced screech-free operation and had a maximum combustion efficiency of 0.92 at a fuel-air ratio of 0.30. At a pressure level of 760 pounds per square foot absolute, a combustion efficiency of 0.77 was obtained at a fuel-air ratio of 0.037. The increase in combustion efficiency of about 0.05 is attributed to the reduction of whirl and the resultant change in diffuser flow conditions.

As shown in figure 18(a), the diffuser total-pressure losses varied from about 0.080 at an altitude of 10,000 feet to about 0.094 at an altitude of 45,000 feet. Thus the increase in diffuser loss was about 0.06 as a result of the installation of the antiwhirl vanes. The large pressure drop across the vanes is probably caused by the high angles of attack and turning necessary in a single stage of flow-straightening vanes and by compromises made in the design to facilitate quick fabrication. The over-all burner total-pressure losses, greatest for configuration 8 because of the upstream location of the flame holder where the average velocity was about 530 feet per second, reached a value of 0.161 at an exhaust-gas temperature of 3000° R compared with the original loss of 0.082 at an altitude of 10,000 feet (fig. 18(b)). Configurations 6 and 7 exhibited 0.03 less over-all total-pressure loss than configuration 8.

The performance of configurations 6, 7, and 8 at an altitude of 10,000 feet and a flight Mach number of 0.49 in terms of augmented thrust ratio and specific fuel consumption, as shown in figure 19, was poorer than that of configuration 1 because of the higher total-pressure losses. If the loss incurred by the vanes had been taken into account in the unaugmented performance, these thrust ratios would be substantially higher. As a result of using the larger exhaust nozzle, augmented thrust ratios were as much as 10 percent greater at the expense of specific fuel consumption. Because elimination of both the severe whirl and the velocity patterns did improve the combustion efficiency, it is evident that the over-all performance could be improved over the performance of configuration 1 by the development of a antiwhirl vane assembly having a lower pressure loss.

CONCLUDING REMARKS

The performance of eight afterburner configurations on a turbojet engine has been presented for a range of fuel-air ratios at various simulated flight conditions. Diffuser-inlet total pressures varied from 4210 to 760 pounds per square foot absolute. Surveys at the afterburner inlet showed that average gas velocities as high as 490 feet per second and whirl angles up to 30° existed. The best afterburner configuration of five tested in the presence of these inlet conditions had a maximum combustion efficiency of 0.87 at an afterburner-inlet pressure of 4210 pounds per square foot absolute and decreased to 0.70 at a pressure level of 760 pounds per square foot absolute. Installation of full-passage antiwhirl vanes at the diffuser inlet reduced the whirl to less than 10°. The performance of the configurations having the reduced whirl showed that an increase in combustion efficiency of about 0.05 was attained. The increased combustion efficiency, however, was offset by increased pressure losses caused by the antiwhirl vanes

with the result that the specific fuel consumption was higher than that of the configuration tested with the higher whirl.

Lewis Flight Propulsion Laboratory
National Advisory Committee for Aeronautics
Cleveland, Ohio, July 20, 1954

APPENDIX A

SYMBOLS

The following symbols are used in this report:

A	area, sq ft
B	thrust-scale reading, lb
C_v	velocity coefficient, ratio of scale jet thrust to exhaust-nozzle rake thrust
D	external drag of installation, lb
F	thrust, lb
f/a	fuel-air ratio
g	gravitational constant, 32.2 ft/sec^2
H	total enthalpy, Btu/lb
M	Mach number
P	total pressure, lb/sq ft abs
p	static pressure, lb/sq ft abs
R	gas constant, 53.4 ft-lb/(lb)(^oR)
T	total temperature, ^oR
V	velocity, ft/sec
W	flow, lb/sec
γ	ratio of specific heats
η	combustion efficiency

Subscripts:

a	air
b	afterburner

e	engine
f	fuel
i	indicated
j	jet
n	net
s	scale
st	standard or unaugmented
t	total
v	venturi station in inlet-air duct
x	inlet duct at frictionless slip joint
0	free-stream conditions
1	engine inlet
4	diffuser inlet (turbine outlet)
5	diffuser outlet (afterburner inlet)
6	exhaust-nozzle inlet

APPENDIX B

METHODS OF CALCULATION

Air flow. - Engine-inlet air flow was obtained by using the pressure measurements at a 26-inch-diameter venturi in the inlet duct and the indicated total temperature at the engine inlet:

$$W_{a,v} = p_v A_v \sqrt{\frac{2\gamma_1 g}{(\gamma_1 - 1)RT_{1,i}} \left(\frac{P_v}{p_v}\right)^{\frac{\gamma_1 - 1}{\gamma_1}} \left[\left(\frac{P_v}{p_v}\right)^{\frac{\gamma_1 - 1}{\gamma_1}} - 1\right]}$$

Compressor and turbine leakages and air extracted for the air-turbine-driven afterburner fuel pump were approximately 2.4 percent of the engine air and were subtracted from engine air flow to obtain the air flow entering the afterburner.

Flight Mach number and airspeed. - The equivalent flight Mach number and airspeed were calculated from the ram-pressure ratio at the inlet of the engine with 100-percent recovery assumed:

$$M_0 = \sqrt{\frac{2}{\gamma_1 - 1}\left[\left(\frac{P_1}{p_0}\right)^{\frac{\gamma_1 - 1}{\gamma_1}} - 1\right]}$$

$$V_0 = M_0 \sqrt{\gamma_1 g R T_{1,i} \left(\frac{p_0}{P_1}\right)^{\frac{\gamma_1 - 1}{\gamma_1}}}$$

Augmented engine thrust. - The jet thrust of the engine and afterburner combination was determined from the thrust-scale reading by the following equation:

$$F_{j,s} = B + D + \frac{W_{a,v} V_x}{g} + A_x(p_x - p_0)$$

The last two terms represent momentum and pressure forces acting at the slip joint on the installation.

The net thrust was obtained by subtracting the inlet momentum term from the jet thrust:

$$F_{n,s} = F_{j,s} - \frac{W_{a,v}V_0}{g}$$

Augmented net-thrust ratio. - The unaugmented jet thrust was calculated by using the total pressures and temperatures at the diffuser inlet (turbine outlet):

$$F_{j,st} = C_v \frac{W_{g,4}}{g} \sqrt{\frac{2gRT_4}{(\gamma_4)(\gamma_4 + 1)}} \left[1 + \gamma_4 - \left(\frac{p_0}{0.94P_4} \right) \left(\frac{\gamma_4 + 1}{2} \right) \frac{\gamma_4}{\gamma_4 - 1} \right]$$

where $W_{g,4} = W_{a,4} + \frac{W_{f,e}}{3600}$, and the velocity coefficient C_v of 0.97 and a diffuser total-pressure loss of 0.06 (total pressure equal to $0.94P_4$) were assumed.

The unaugmented net thrust was:

$$F_{n,st} = F_{j,st} - \frac{W_{a,v}V_0}{g}$$

The augmented thrust ratio was then the ratio of the scale net thrust to the unaugmented net thrust.

Exhaust-gas total temperature. - The total temperature of the exhaust gas was calculated from the exhaust-nozzle total pressure, the scale jet thrust, the velocity coefficient, and the gas flow by means of the following equation:

$$T_j = \left(\frac{F_{j,s}}{W_{g,6}C_v} \right)^2 \frac{g}{2R} \frac{\gamma_6 - 1}{\gamma_6} \frac{1}{\left[1 - \left(\frac{p_0}{P_6} \right) \frac{\gamma_6 - 1}{\gamma_6} \right]}$$

where $W_{g,6} = W_{a,4} + W_{f,t}/3600$, and the velocity coefficient C_v was experimentally determined from nonafterburning operation and varied between 0.95 and 0.98 depending on the nozzle size (original or final) and flight condition.

Combustion efficiency. - The engine combustion efficiency was calculated in a conventional manner. This engine combustion efficiency and the over-all enthalpy rise across the engine and afterburner combination were used in the following equation to calculate the afterburner combustion efficiency:

$$\eta_b = \frac{H_{a,6} - H_{a,1} + (f/a)_t H_{f,6} - \eta_e (f/a)_e (18,700)}{\left(\frac{W_{f,b}/3600}{W_{a,4}}\right)(18,700) + (1 - \eta_e)(f/a)_e (18,700)}$$

where 18,700 Btu per pound is the fuel lower heating value.

Afterburner fuel-air ratio. - Because the air used in the engine combustor is unavailable for combustion in the afterburner, the afterburner fuel-air ratio was the ratio of afterburner fuel flow to unburned air flow as calculated in the following equation:

$$(f/a)_b = \frac{W_{f,b}/3600}{W_{a,4} - 15(W_{f,e}/3600)}$$

where the constant 15 is the stoichiometric air-fuel ratio.

Velocity. - Static and total pressures along with the total temperature were used in the following equation to calculate diffuser velocity:

$$V_5 = \sqrt{\frac{2\gamma_4 g R T_4}{\gamma_4 - 1}\left[1 - \left(\frac{p_5}{P_5}\right)^{\frac{\gamma_4 - 1}{\gamma_4}}\right]}$$

REFERENCES

1. Usow, Karl H., Meyer, Carl L., and Schulze, Frederick W.: Experimental Investigation of Screeching Combustion in Full-Scale Afterburner. NACA RM E53I01, 1953.

2. Braithwaite, Willis M., Renas, Paul E., and Jansen, Emmert T.: Altitude Investigation of Three Flame-Holder and Fuel-Systems Configurations in a Short Converging Afterburner on a Turbojet Engine. NACA RM E52G29, 1952.

3. Conrad, E. William, Schulze, Frederick W., and Usow, Karl H.: Effect of Diffuser Design, Diffuser-Exit Velocity Profile, and Fuel Distribution on Altitude Performance of Several Afterburner Configurations. NACA RM E53A30, 1953.

4. Henzel, James L., Jr., and Bryant, Lively: Investigation of Effect of Number and Width of Annular Flame-Holder Gutters on Afterburner Performance. NACA RM E54C30, 1954.

TABLE I. - AFTERBURNER CONFIGURATIONS.

Configuration	Diffuser (See fig. 2)		Flame holder (See fig. 3)			Fuel bars[a] (See fig. 4)		Sketch of configurations, fig.
	Inner cone	Vanes or deflectors	Designation	Position	Blockage, percent	Designation	Position	
1	Original	None	A	1	32	A	1	1
2	Original	None	A	1	32	A	3	1
3	Pilot step	None	A	3	29	B	1	8
4	Original	Deflectors	A	2	32	C	1	8
5	Long	None	B	4	35	A	2	8
6	Long	Vanes	C	4	37	D	4	16
7	Long	Vanes	D	4	36	A E	2 4	16
8	Original	Vanes	B	1	39	F	1	16

[a]20 in number equally spaced around circumference.

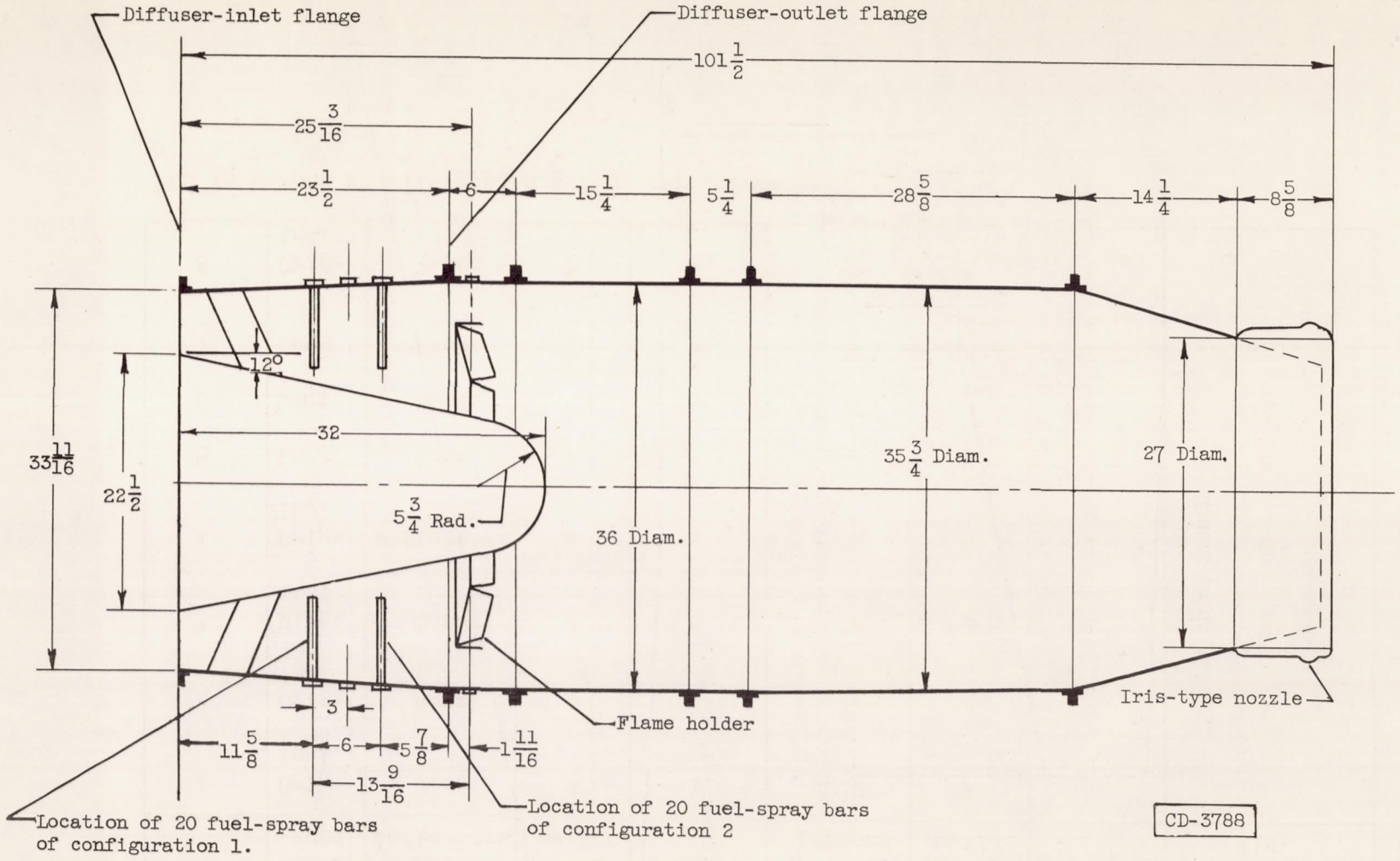

Figure 1. - Details of afterburner configurations 1 and 2. (All dimensions in inches.)

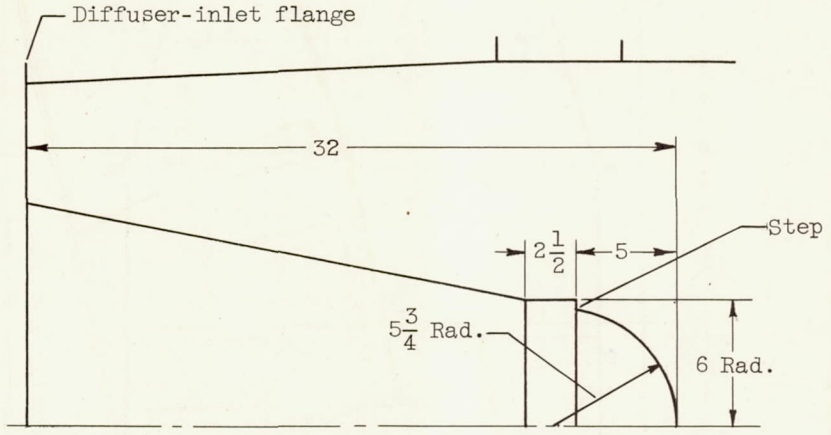

(a) Details of pilot-type step added to original inner cone. (All dimensions in inches.)

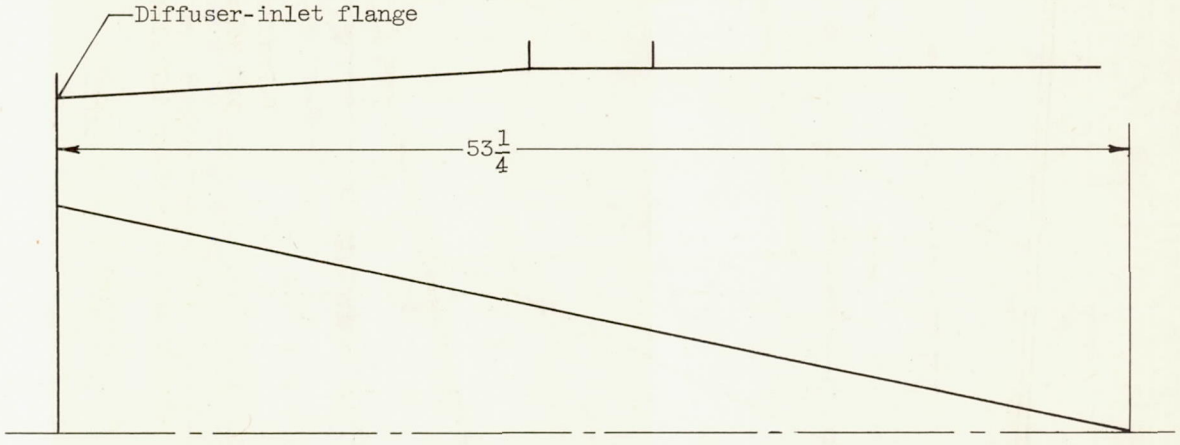

(b) Details of extended inner cone. (All dimensions in inches.)

CD-3789

Figure 2. - Diffuser modifications.

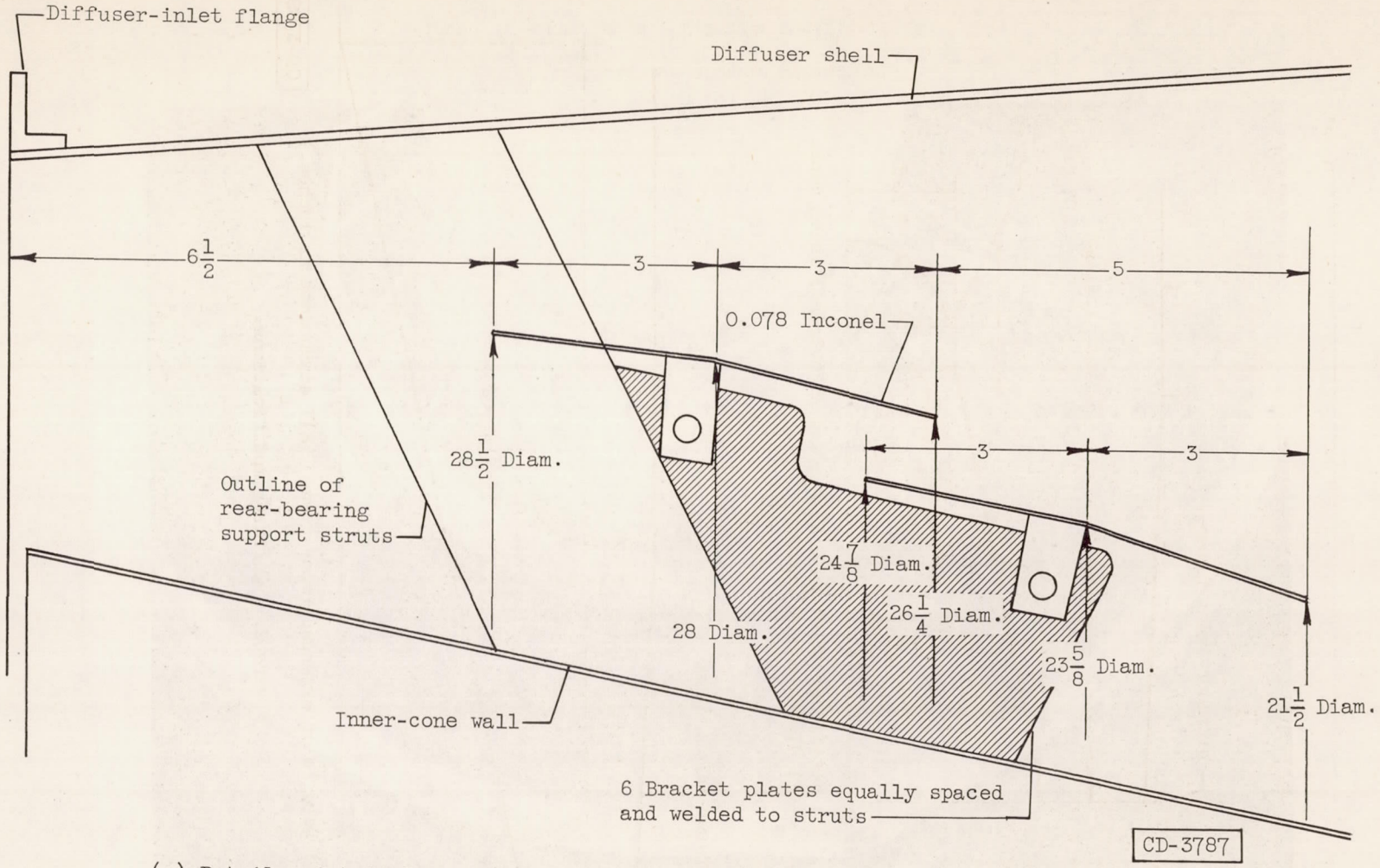

(c) Details of twin-deflector cascade installed in diffuser. (All dimensions in inches.)

Figure 2. - Continued. Diffuser modifications.

CONFIDENTIAL

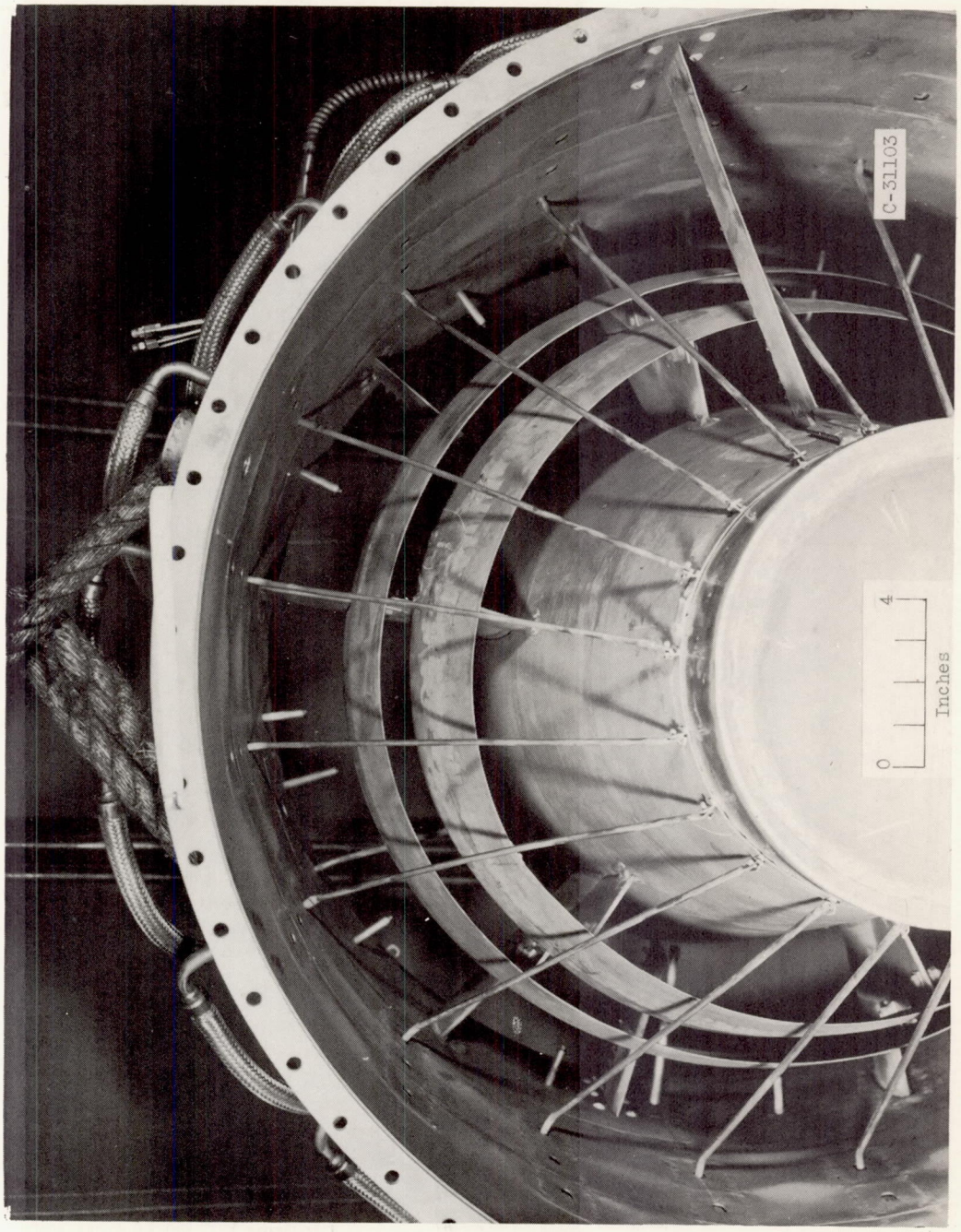

(d) Installation of twin deflectors.

Figure 2. - Continued. Diffuser modifications.

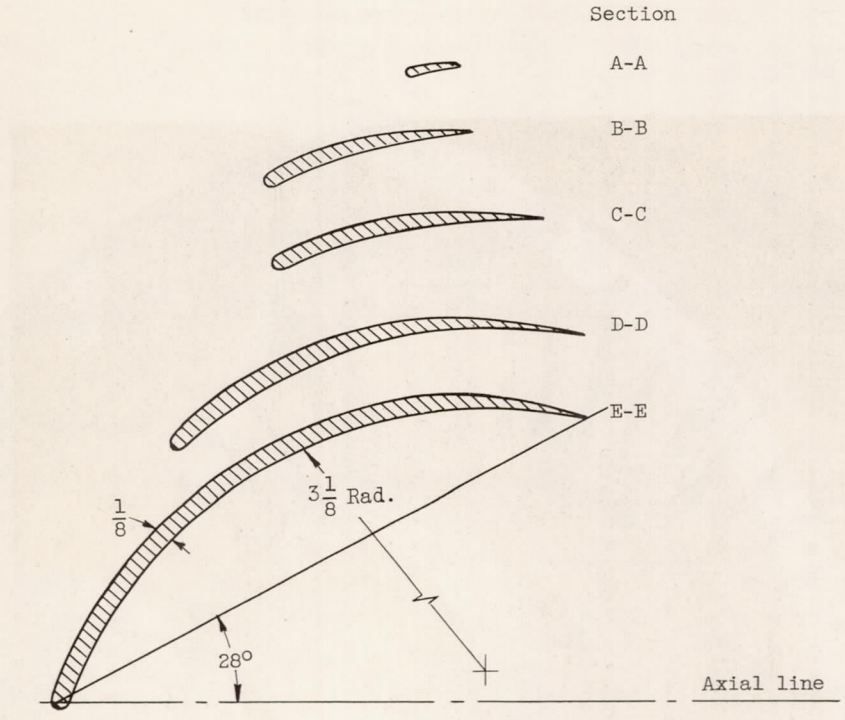

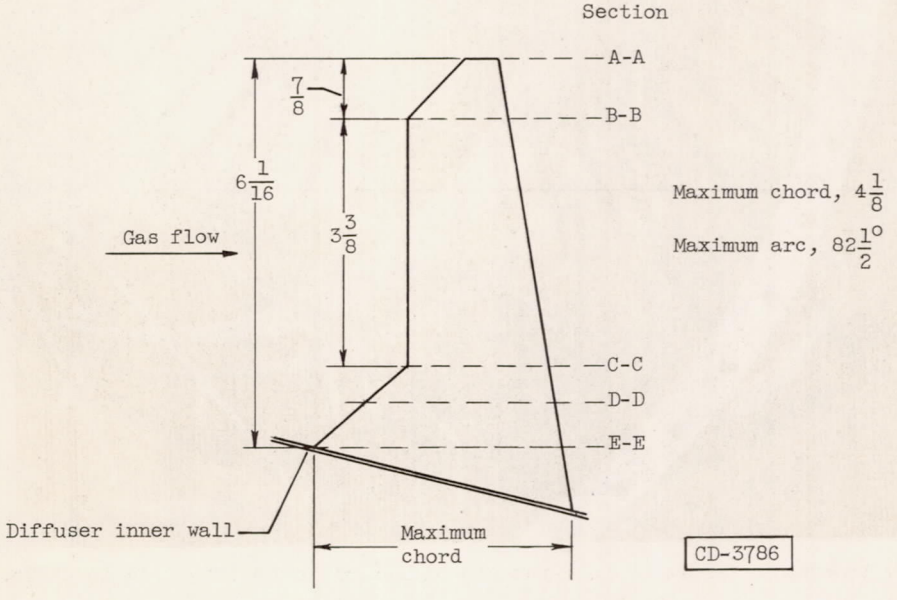

(e) Details of 48 full-passage antiwhirl vanes. (All dimensions in inches.)

Figure 2. - Continued. Diffuser modifications.

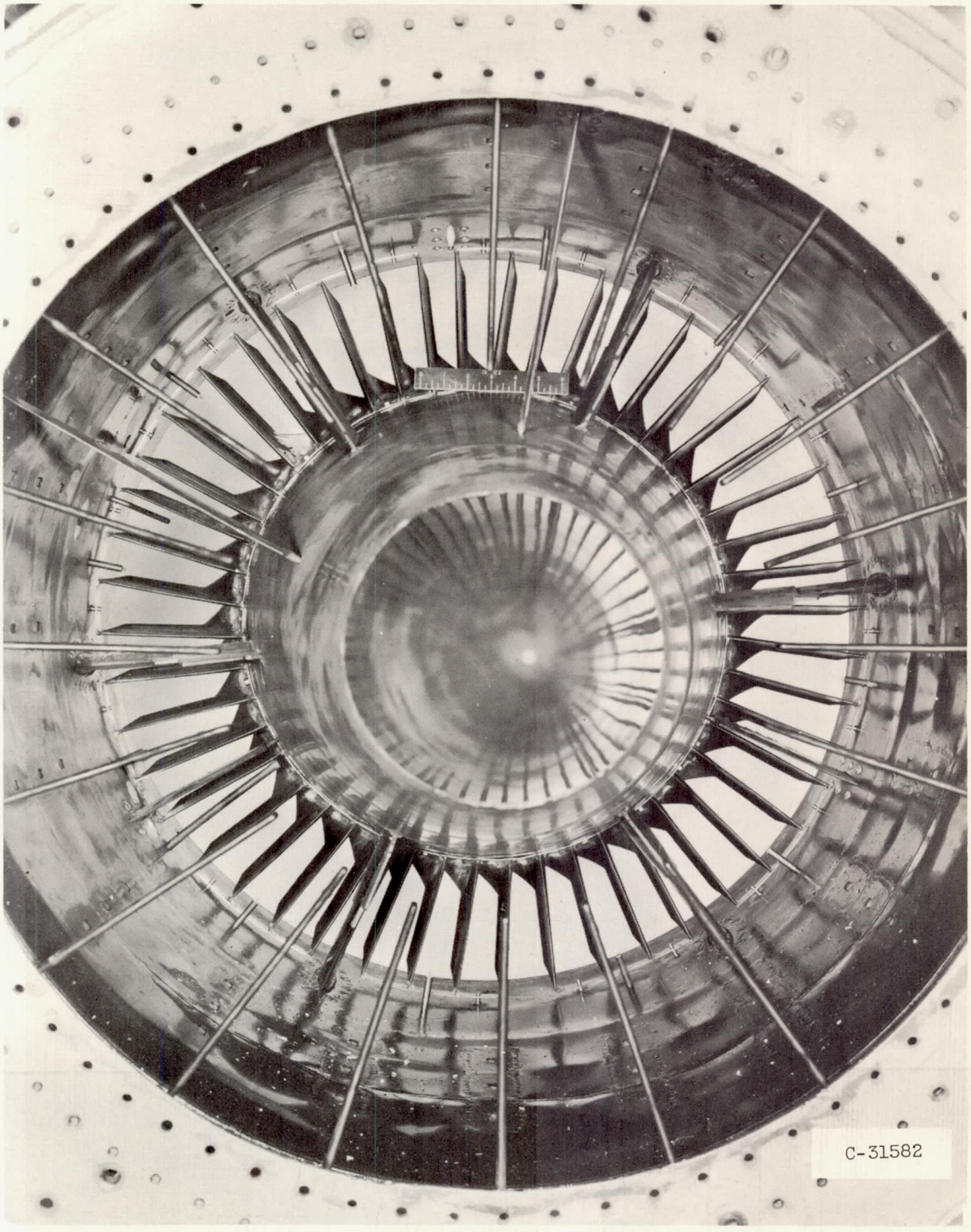

(f) View looking upstream of full-passage antiwhirl vanes installed in diffuser.

Figure 2. - Concluded. Diffuser modifications.

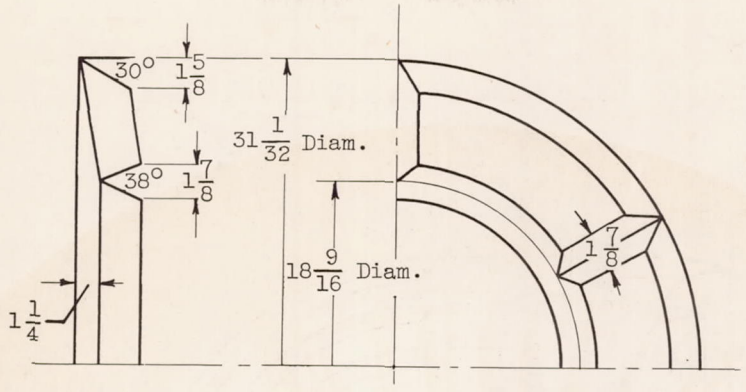

(a) Flame holder A. Blocked area, 300 square inches.

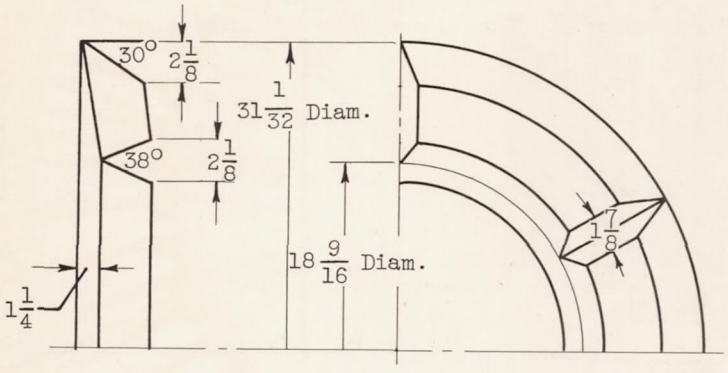

(b) Flame holder B. Blocked area, 357.5 square inches.

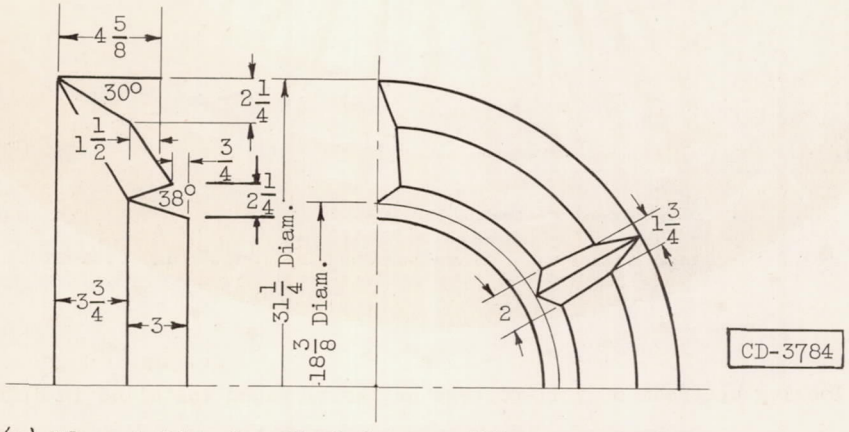

(c) Flame holder C. Blocked area, 376 square inches.

Figure 3. - Flame holders and flame-holder positions. (All dimensions in inches.)

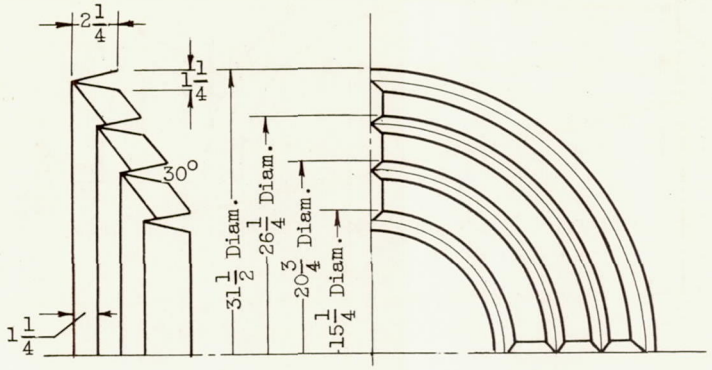

(d) Flame holder D. Blocked area, 366.5 square inches.

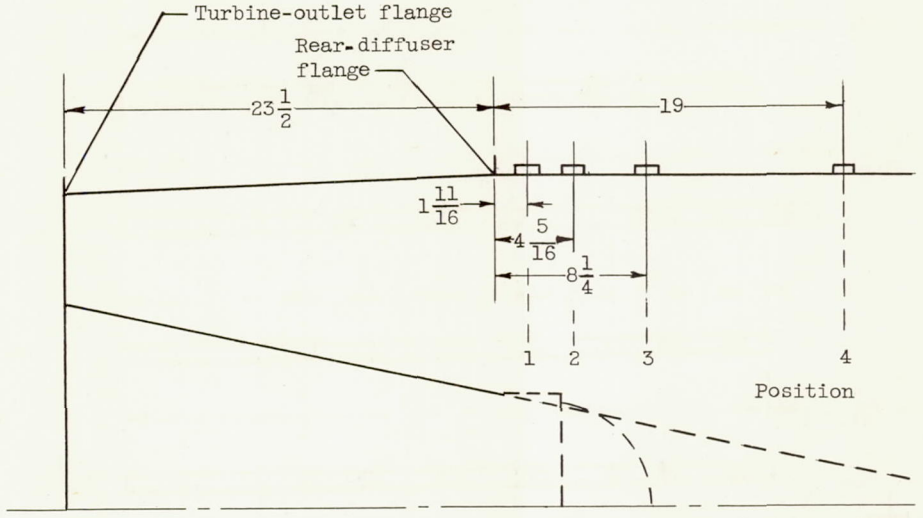

(e) Flame-holder positions.

CD-3785

Figure 3. - Concluded. Flame holders and flame-holder positions. (All dimensions in inches.)

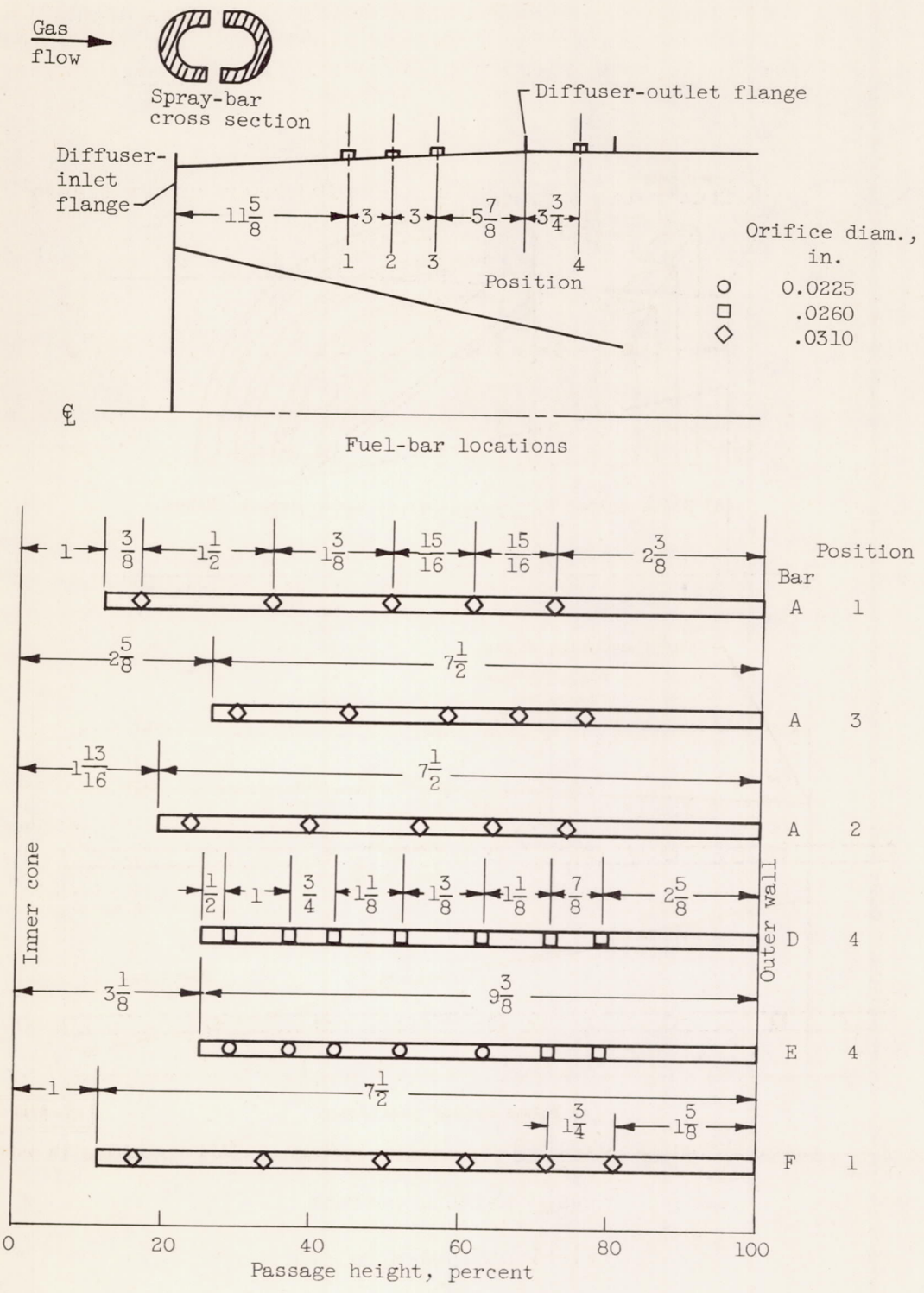

(a) Radial fuel-spray bars.

Figure 4. - Details of fuel-spray bars. (All dimensions in inches.)

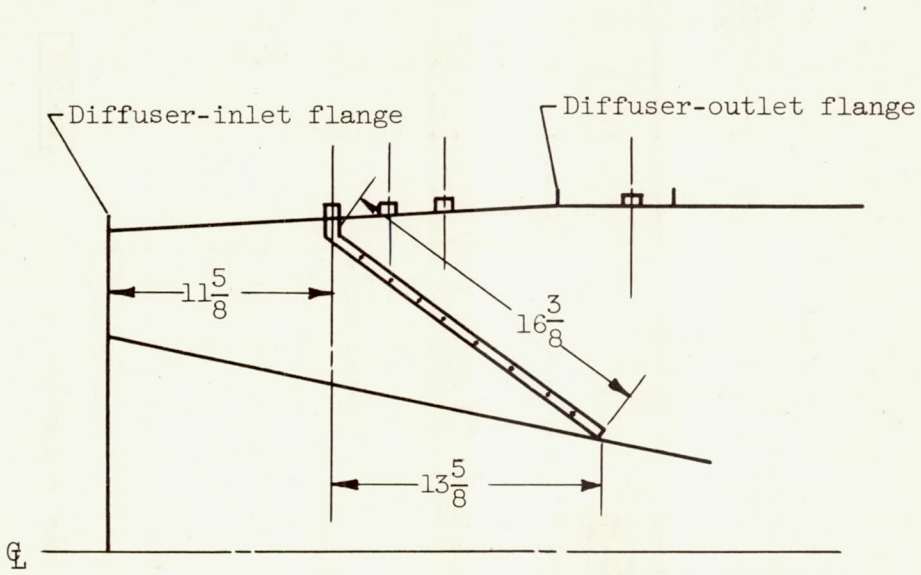

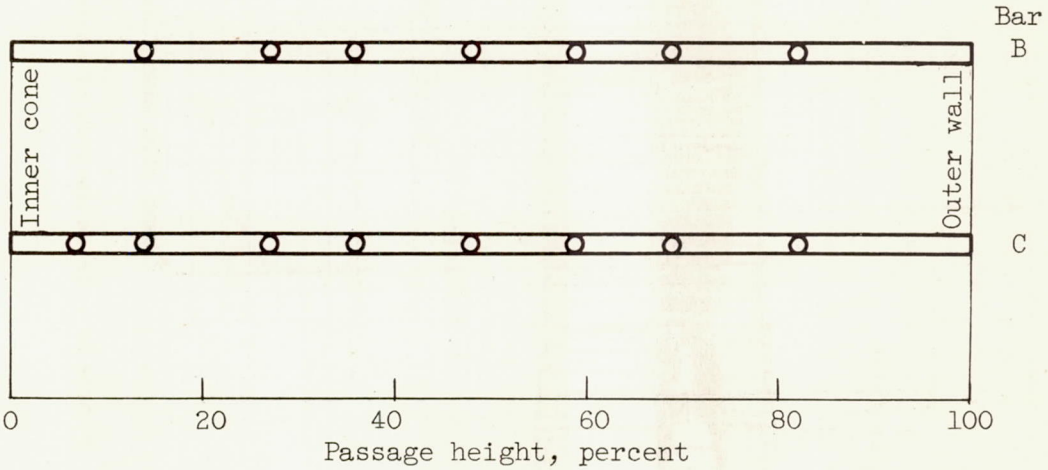

(b) Slant fuel-spray bars.

Figure 4. - Concluded. Details of fuel-spary bars. (All dimensions in inches.)

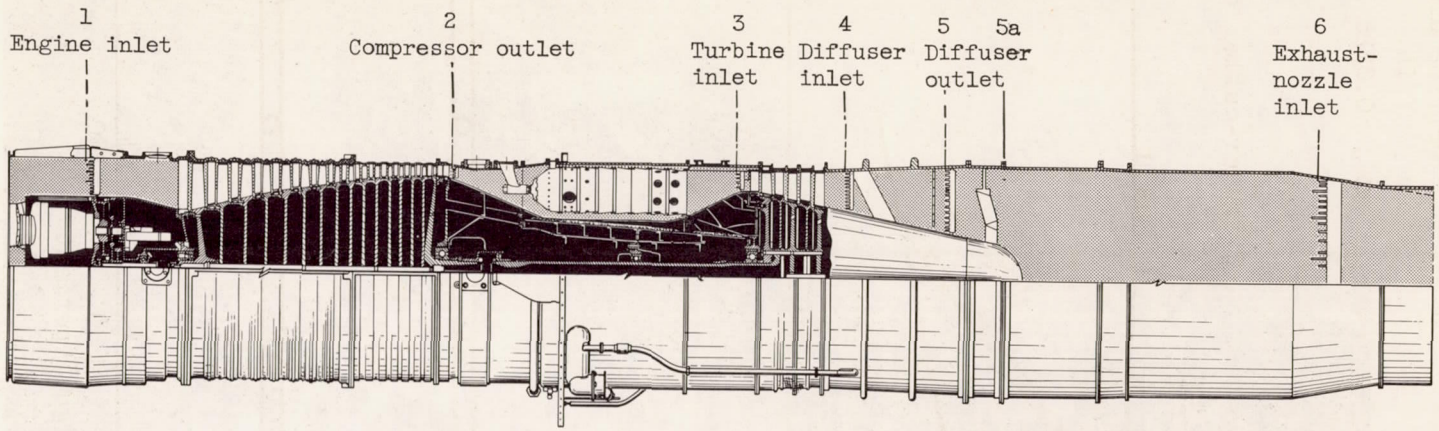

Station	Pressure tubes			Thermocouples
	Total	Stream static	Wall static	
1	28	8	4	6
2	8	1	0	8
3	8	0	0	4
4	21	0	6	18
5	14	0	4	0
5 and [a]5a	12	0	2	0
6	20	4	2	0

[a]Used only when flame holder was downstream of station.

CD-3030

Figure 5. - Cross section of engine and afterburner showing instrumentation locations.

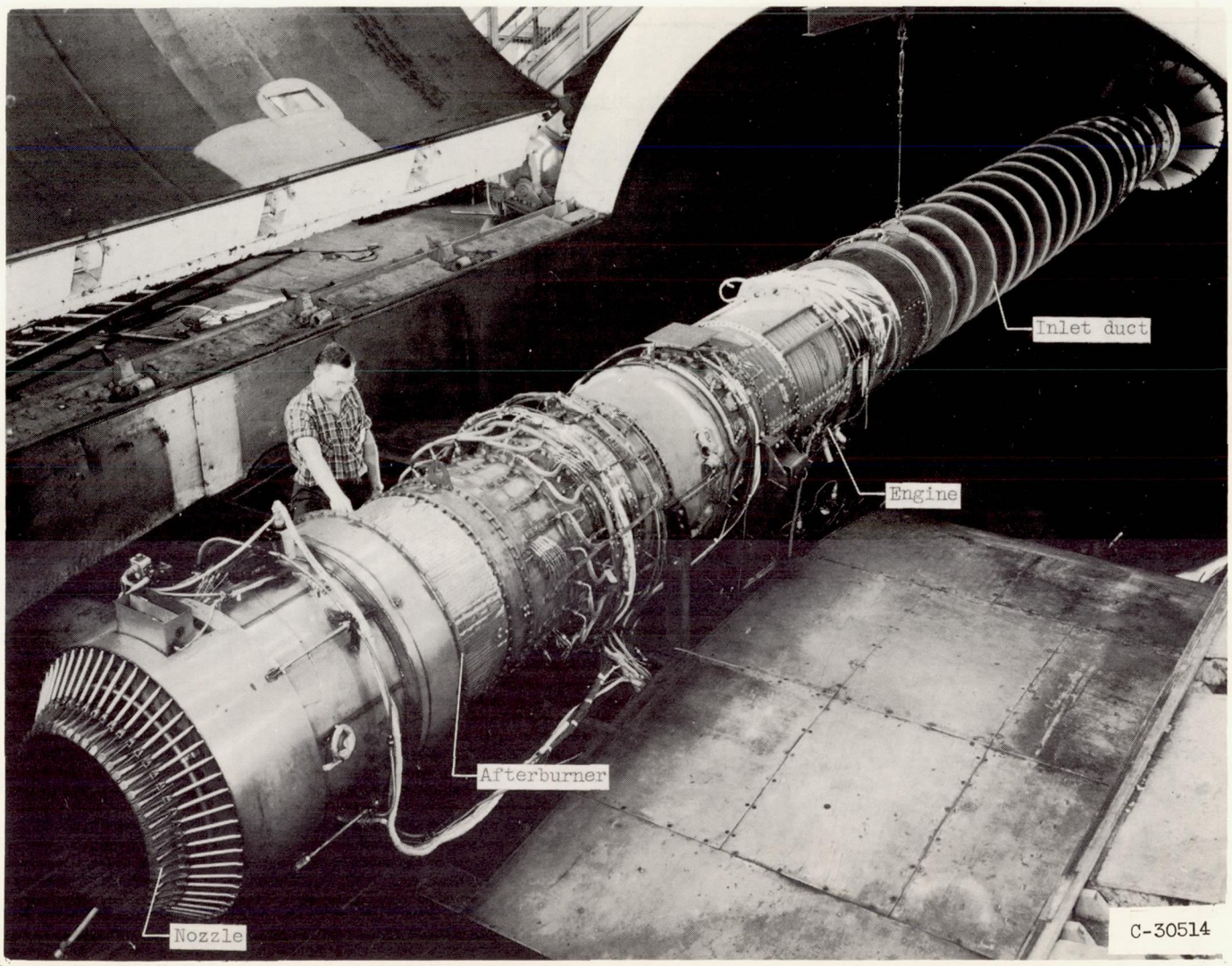

Figure 6. - Engine and afterburner installation in altitude wind tunnel.

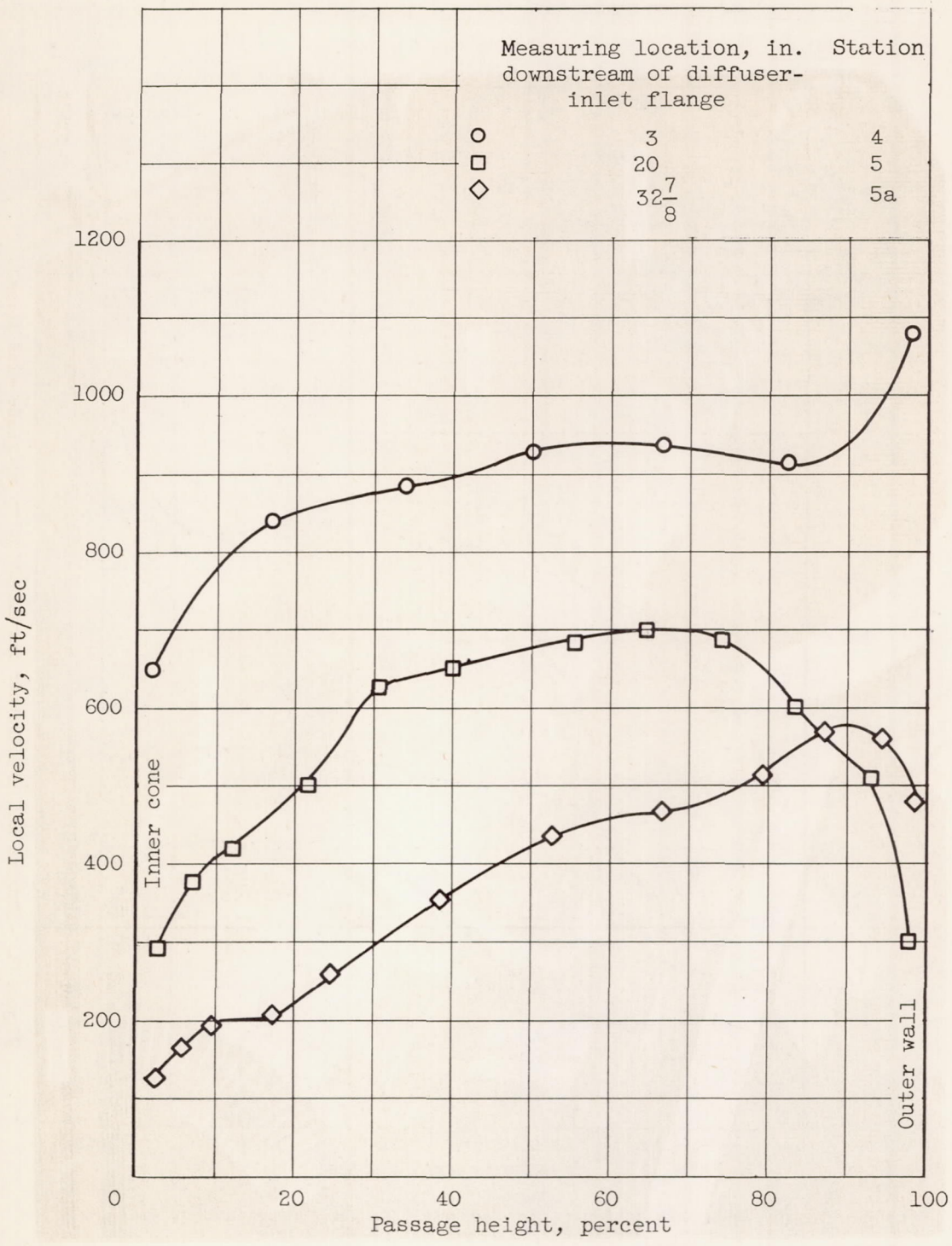

(a) Velocity profiles. Altitude, 35,000 feet; flight Mach number, 1.00.

Figure 7. - Afterburner-inlet flow conditions.

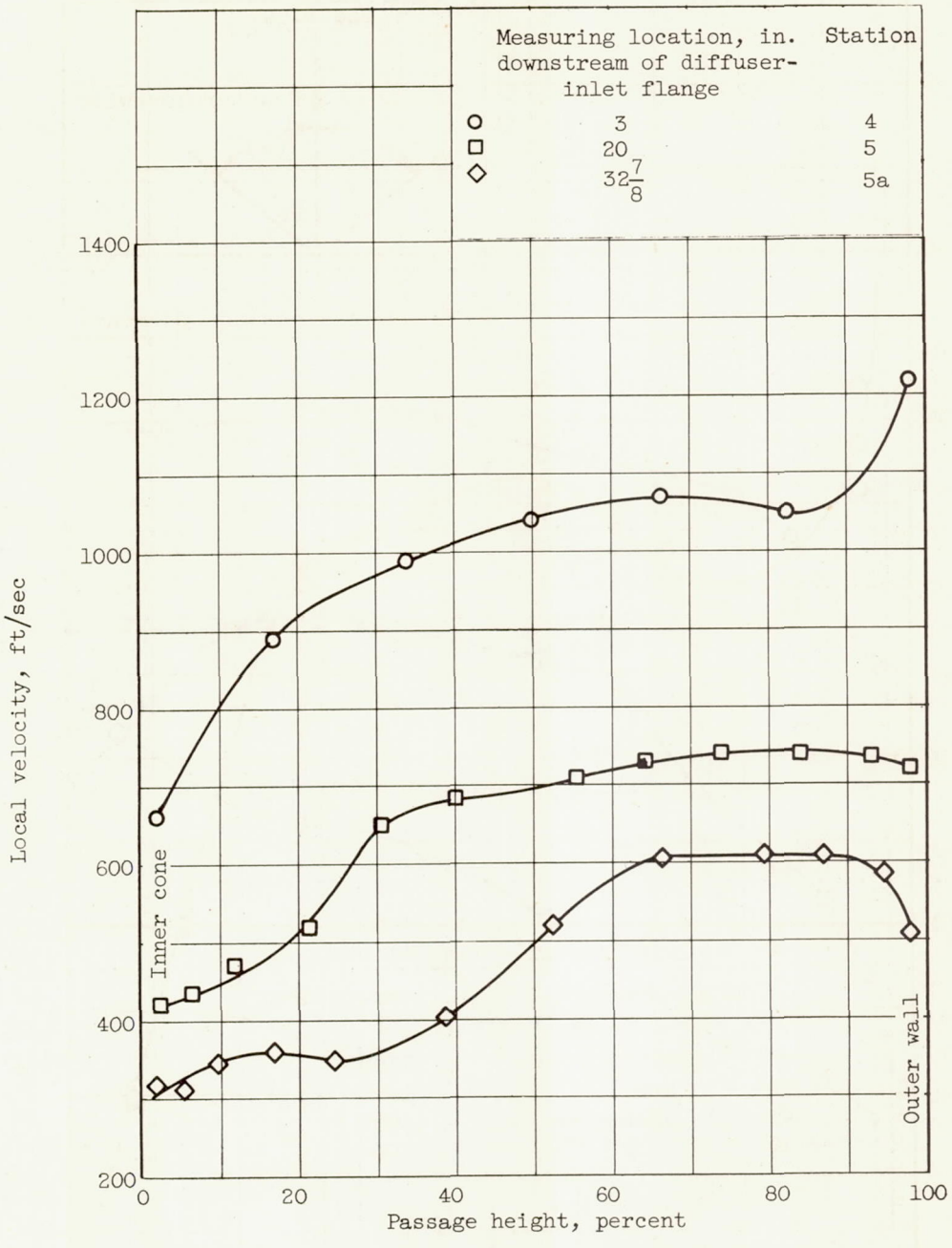

(b) Velocity profiles. Altitude, 45,000 feet; flight Mach number, 0.15.

Figure 7. - Continued. Afterburner-inlet flow conditions.

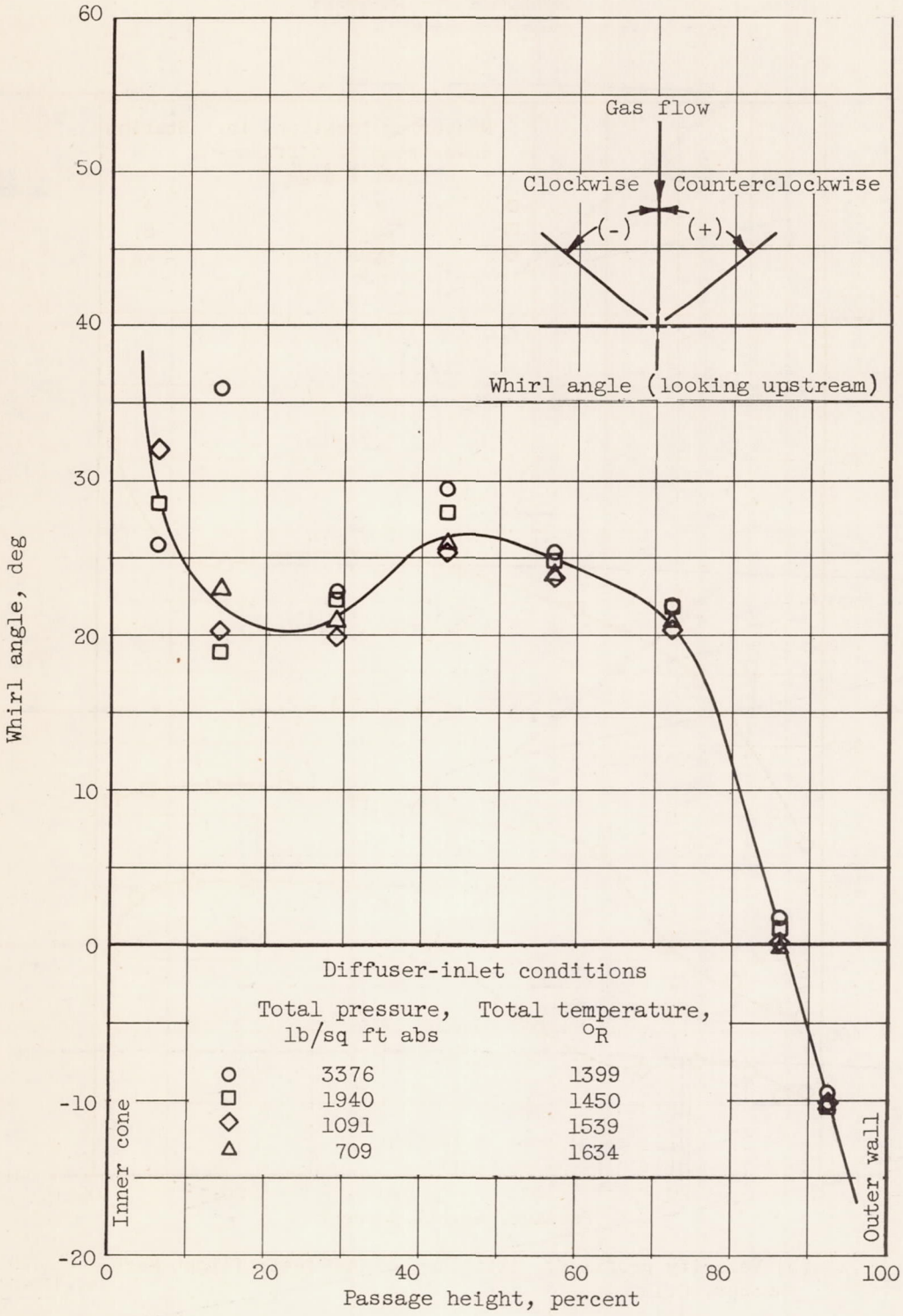

(c) Whirl pattern $5\frac{1}{2}$ inches downstream of diffuser inlet.

Figure 7. - Concluded. Afterburner-inlet flow conditions.

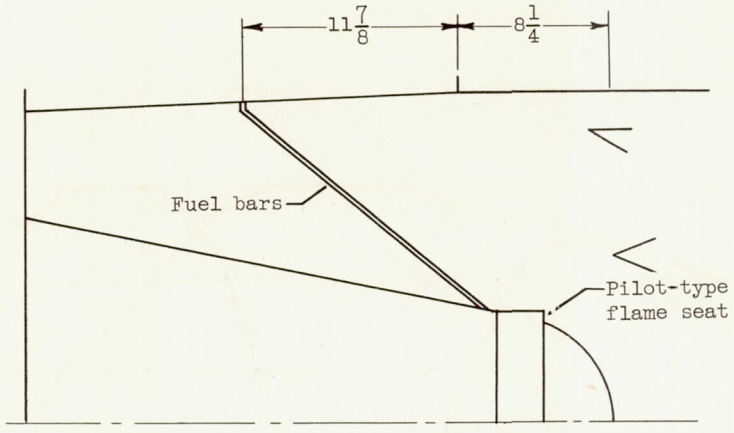

(a) Configuration 3.

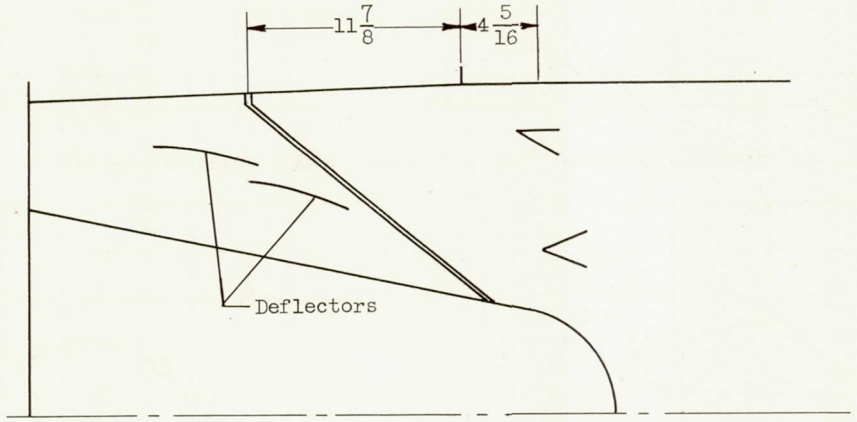

(b) Configuration 4.

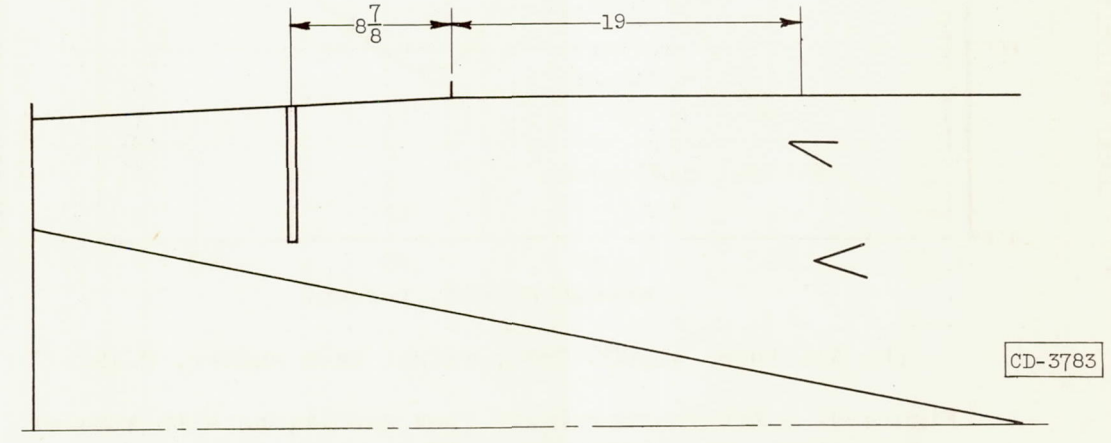

(c) Configuration 5.

Figure 8. - Schematic sketches of configurations 3, 4, and 5. (All dimensions in inches.)

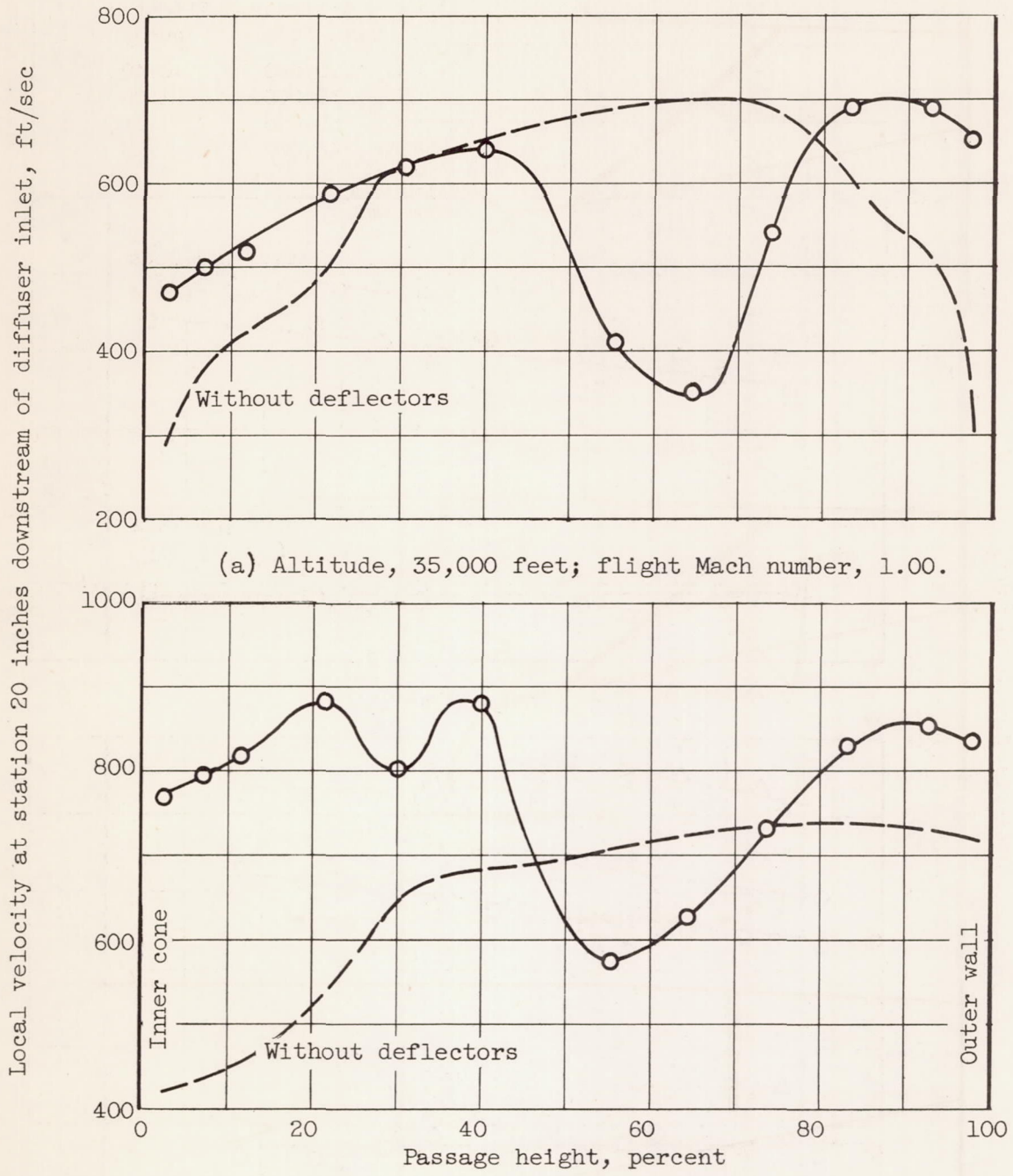

(a) Altitude, 35,000 feet; flight Mach number, 1.00.

(b) Altitude, 45,000 feet; flight Mach number, 0.15.

Figure 9. - Afterburner-inlet flow conditions with annular deflectors installed.

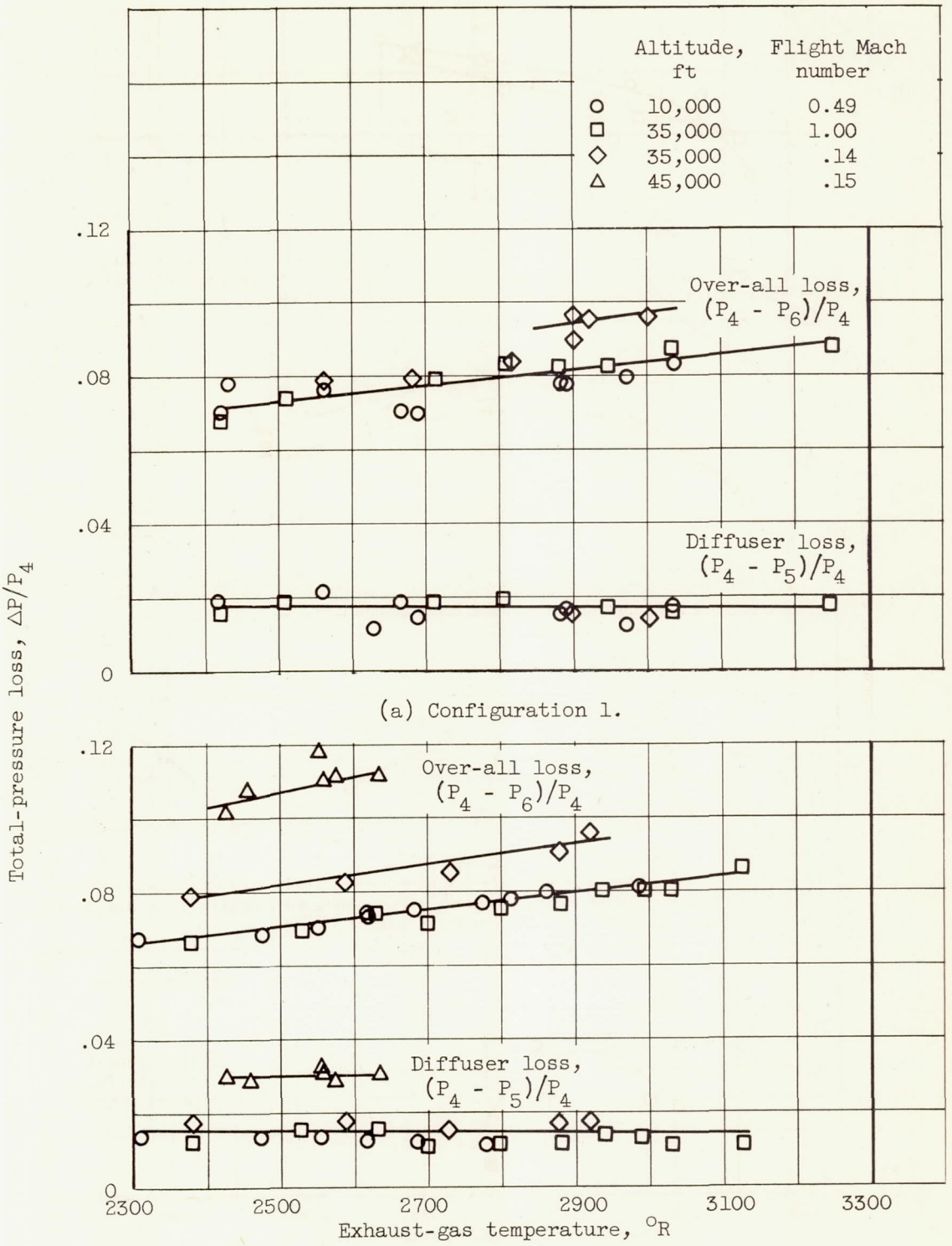

(a) Configuration 1.

(b) Configuration 2.

Figure 10. - Total-pressure losses of configurations 1 and 2.

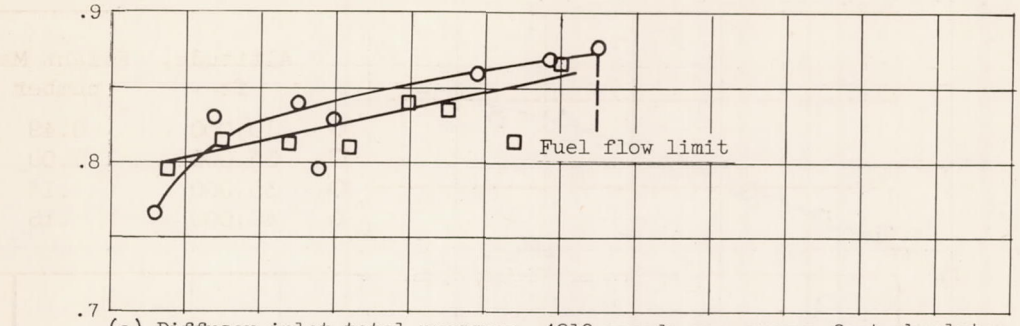

(a) Diffuser-inlet total pressure, 4210 pounds per square foot absolute; altitude, 10,000 feet; flight Mach number, 0.49.

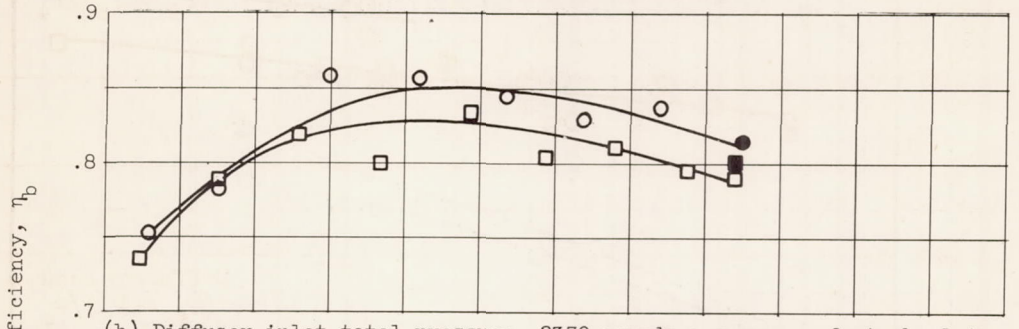

(b) Diffuser-inlet total pressure, 2370 pounds per square foot absolute; altitude, 35,000 feet; flight Mach number, 1.00.

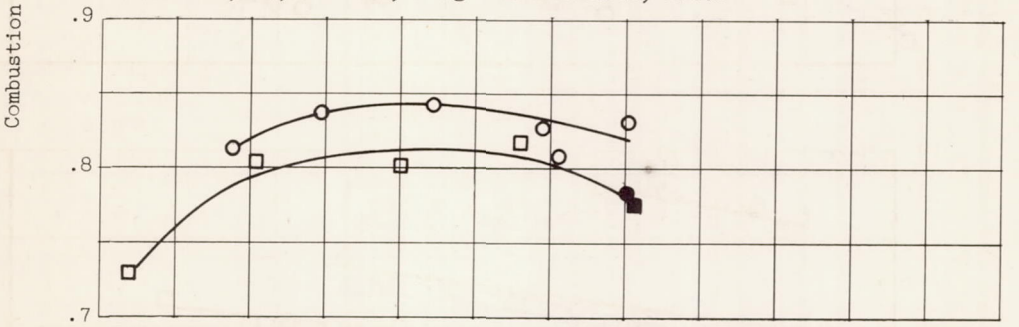

(c) Diffuser-inlet total pressure, 1250 pounds per square foot absolute; altitude, 35,000 feet; flight Mach number, 0.14.

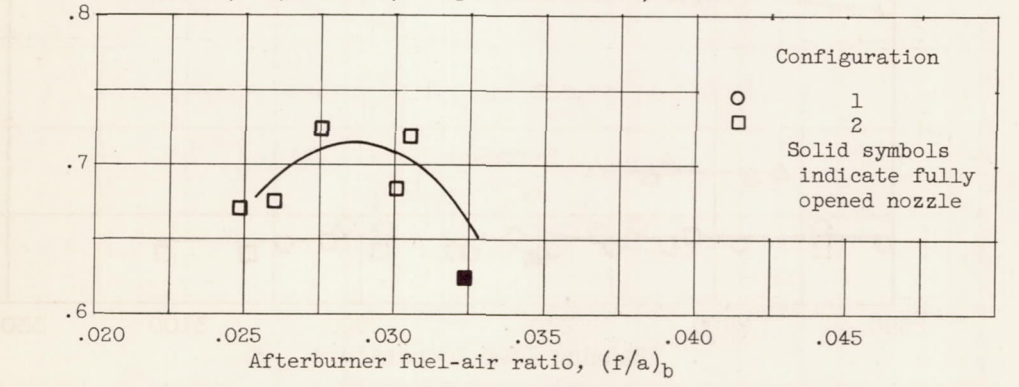

(d) Diffuser-inlet total pressure, 760 pounds per square foot absolute; altitude, 45,000 feet; flight Mach number, 0.15.

Figure 11. - Combustion efficiencies of configurations 1 and 2.

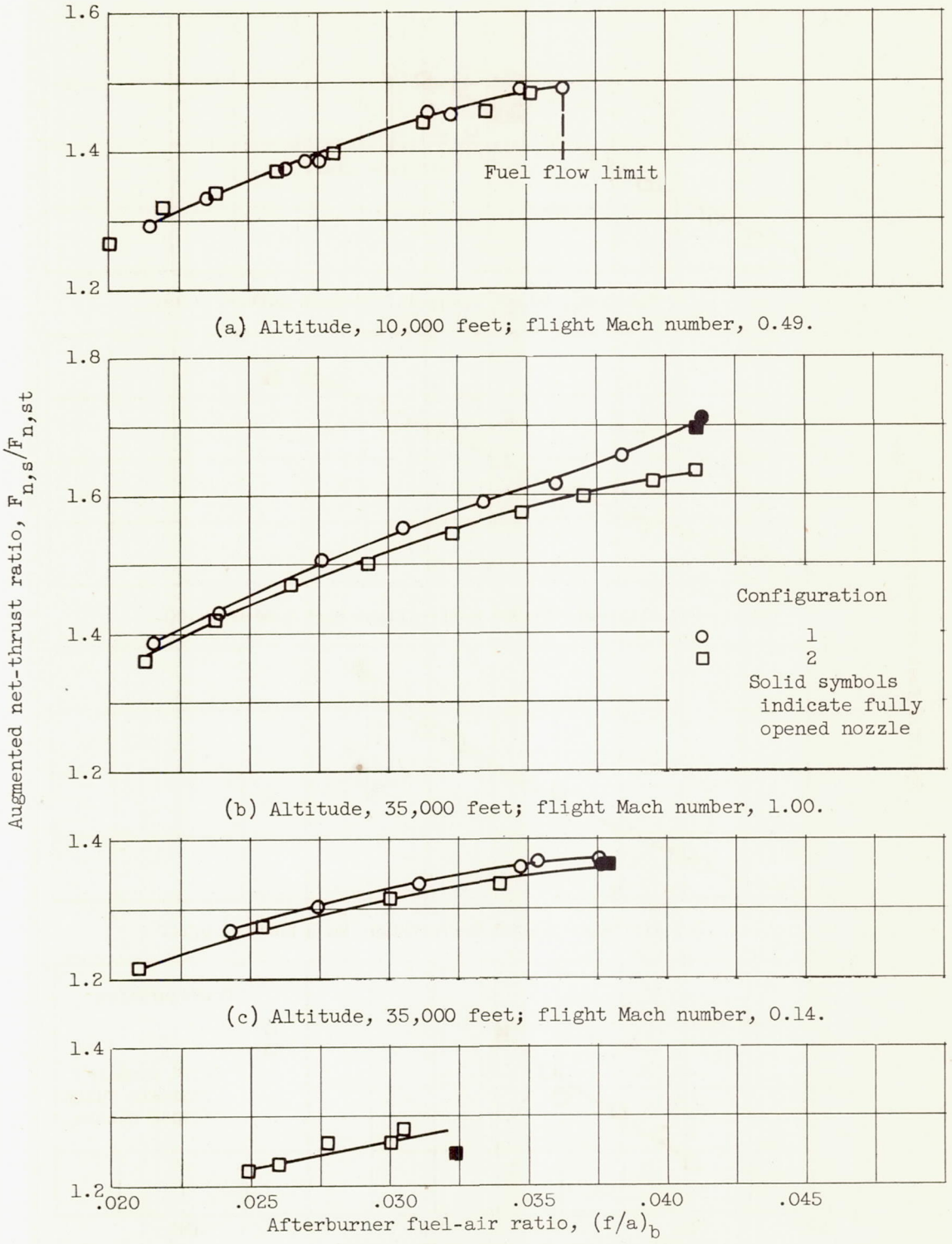

Figure 12. - Augmented thrust ratios of configurations 1 and 2.

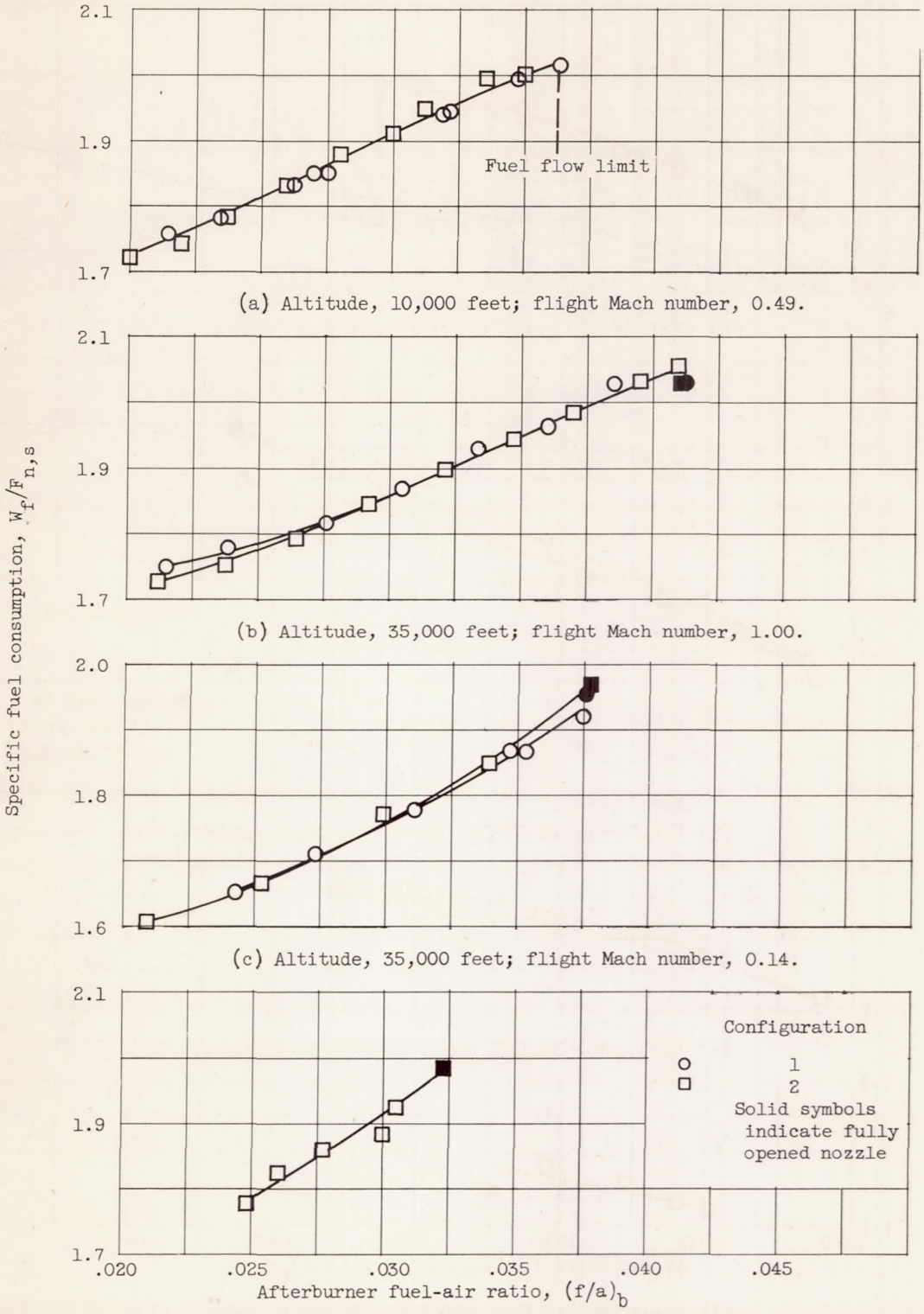

(a) Altitude, 10,000 feet; flight Mach number, 0.49.

(b) Altitude, 35,000 feet; flight Mach number, 1.00.

(c) Altitude, 35,000 feet; flight Mach number, 0.14.

(d) Altitude, 45,000 feet; flight Mach number, 0.15.

Figure 13. - Specific fuel consumption of configurations 1 and 2.

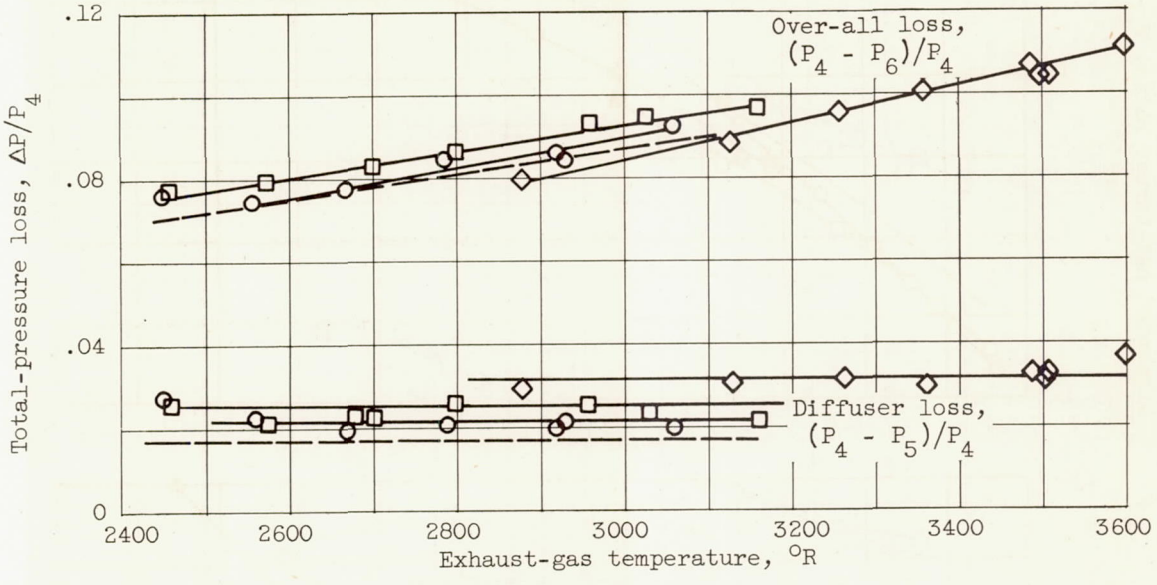

(a) Total-pressure loss.

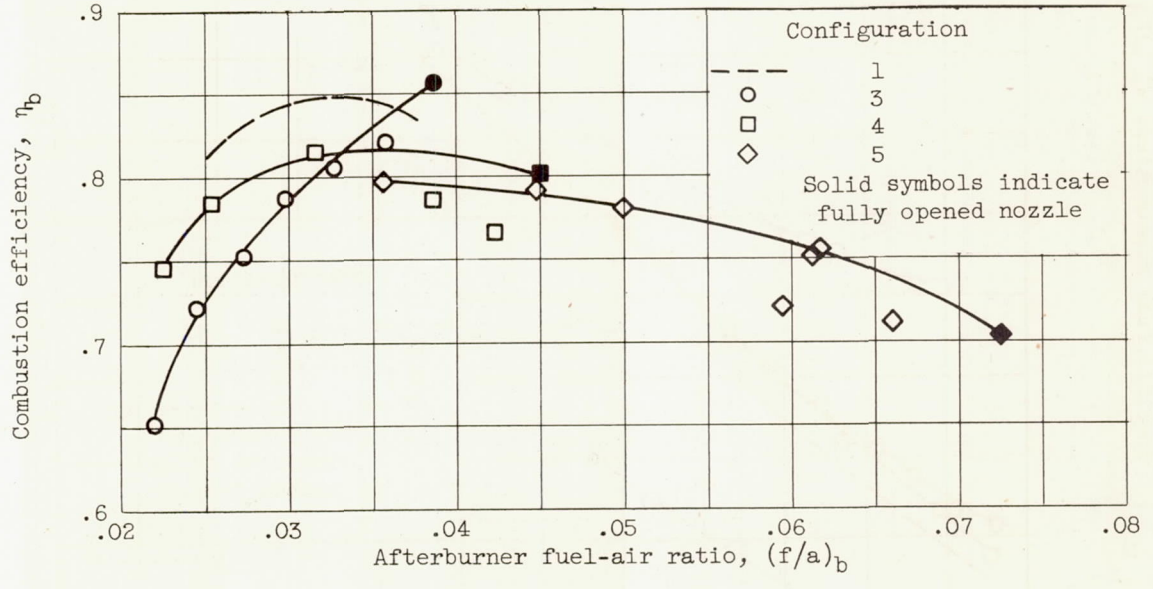

(b) Combustion efficiency.

Figure 14. - Afterburner performance of configurations 3, 4, and 5. Altitude, 35,000 feet; flight Mach number, 1.00.

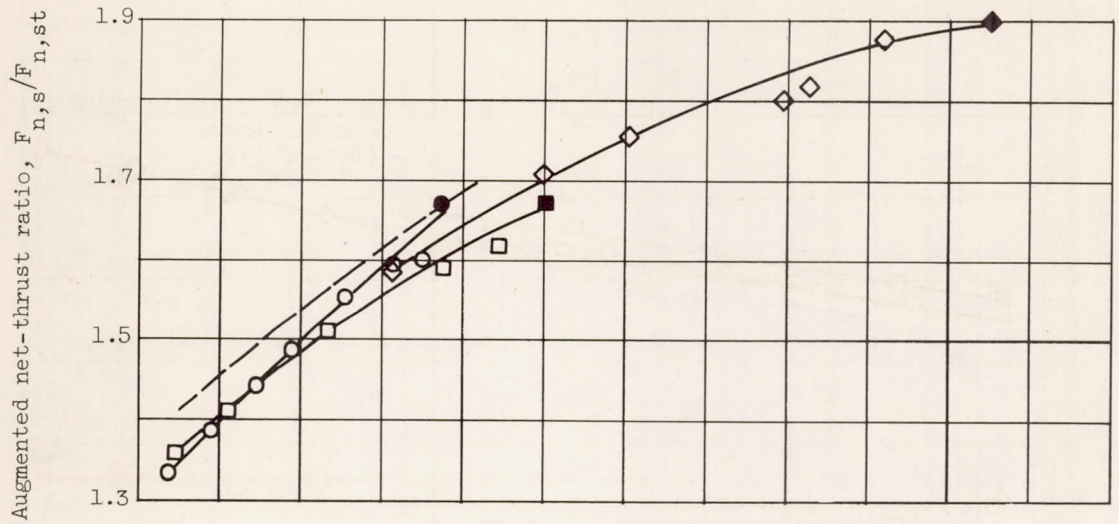

(c) Augmented thrust ratio.

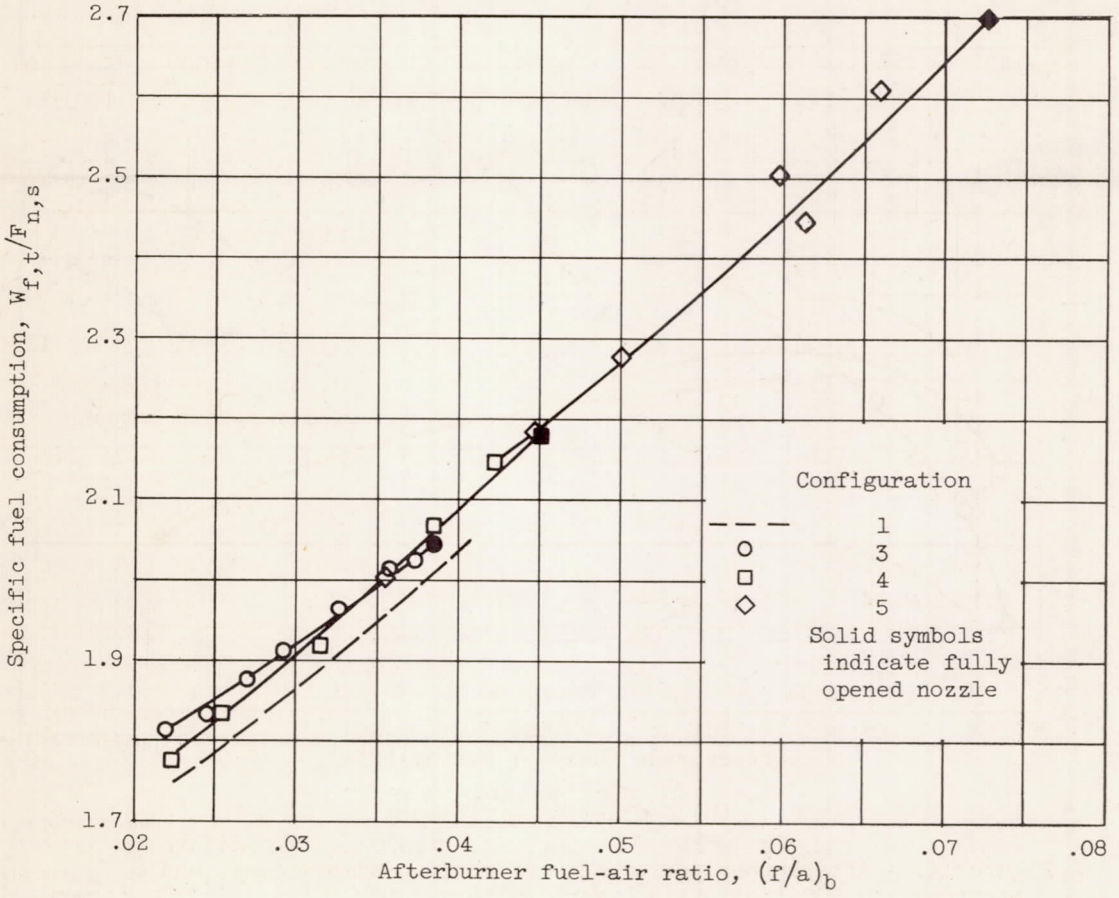

(d) Specific fuel consumption.

Figure 14. - Concluded. Afterburner performance of configurations 3, 4, and 5. Altitude, 35,000 feet; flight Mach number, 1.00.

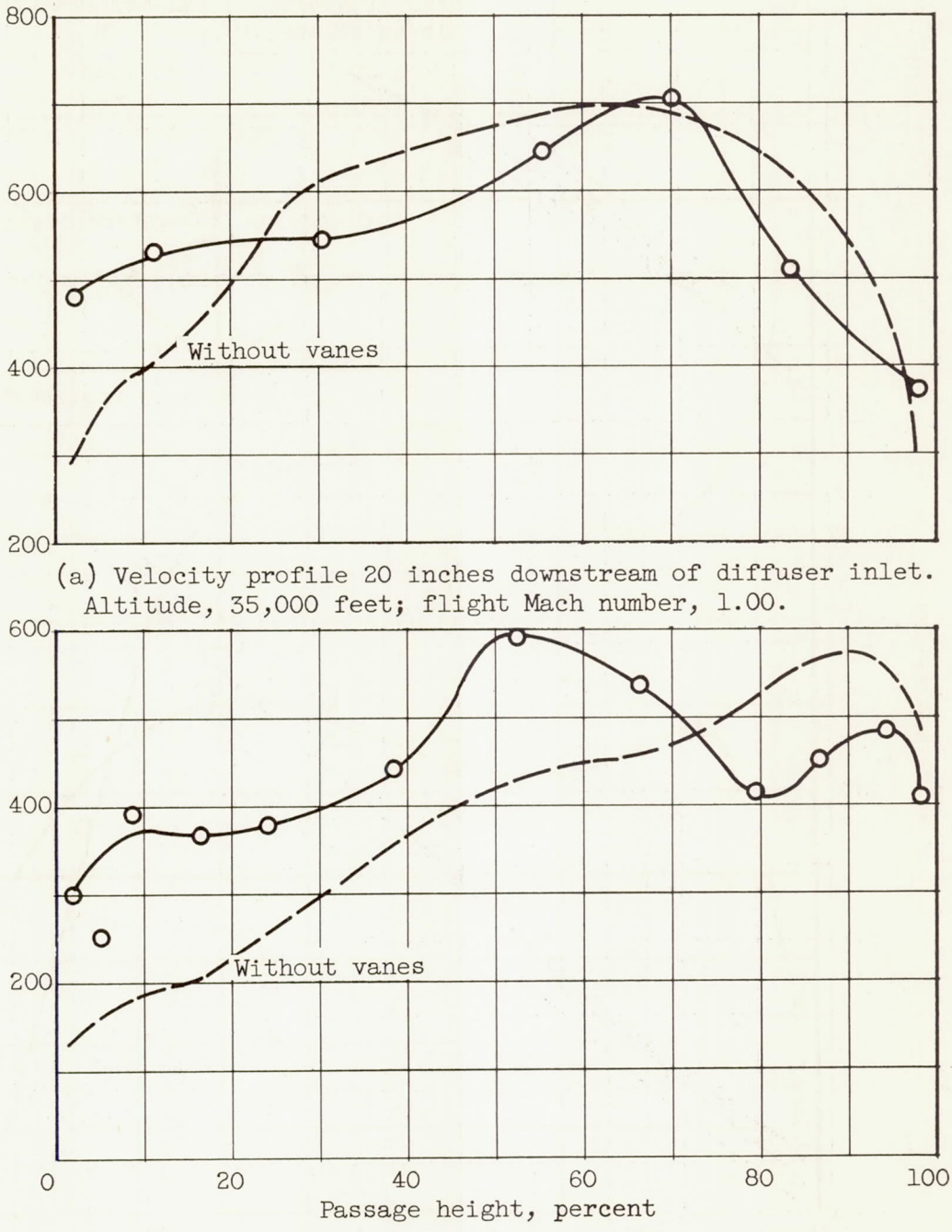

(a) Velocity profile 20 inches downstream of diffuser inlet. Altitude, 35,000 feet; flight Mach number, 1.00.

(b) Velocity profile $32\frac{7}{8}$ inches downstream of diffuser inlet. Altitude, 35,000 feet; flight Mach number, 1.00.

Figure 15. - Afterburner-inlet flow conditions with full-passage antiwhirl vanes.

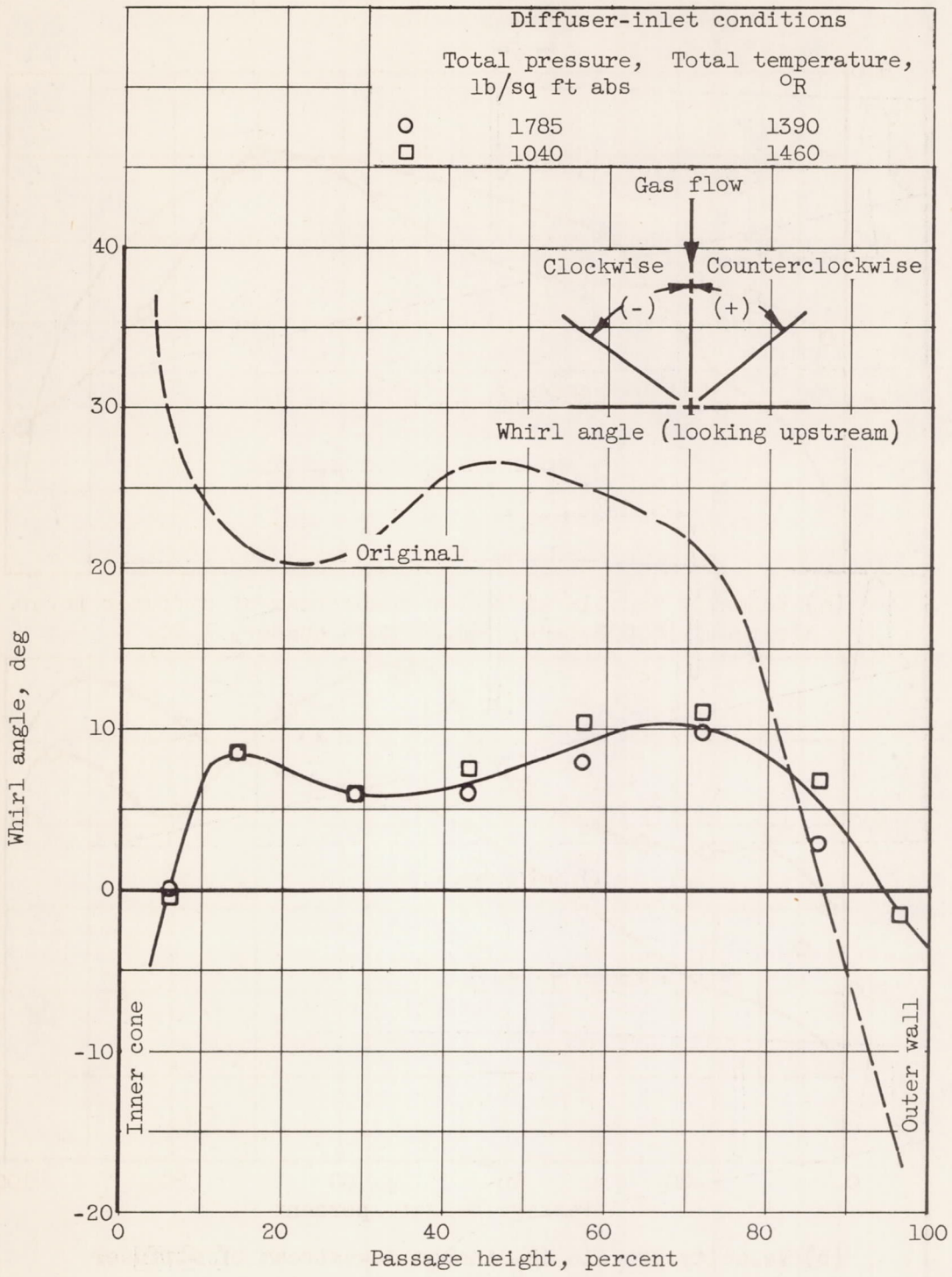

(c) Whirl profile $5\frac{1}{2}$ inches downstream of diffuser inlet.

Figure 15. - Concluded. Afterburner-inlet flow conditions with full-passage antiwhirl vanes.

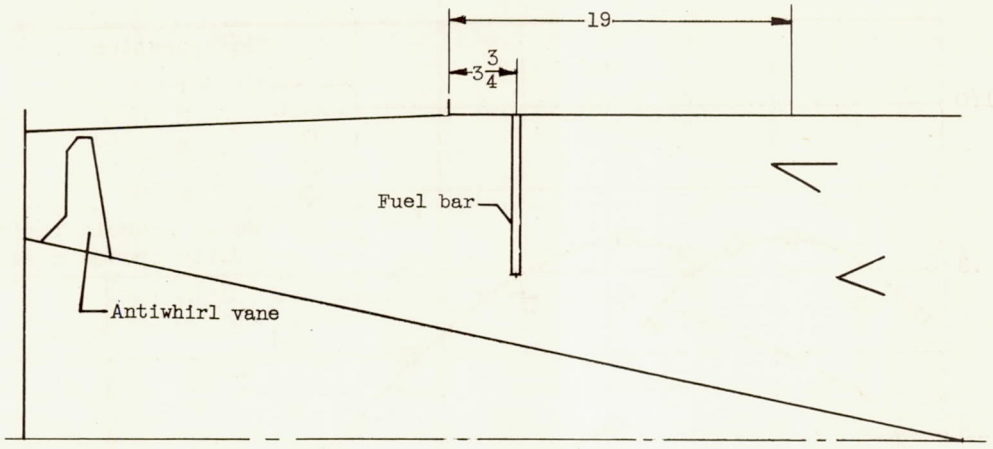

(a) Configuration 6.

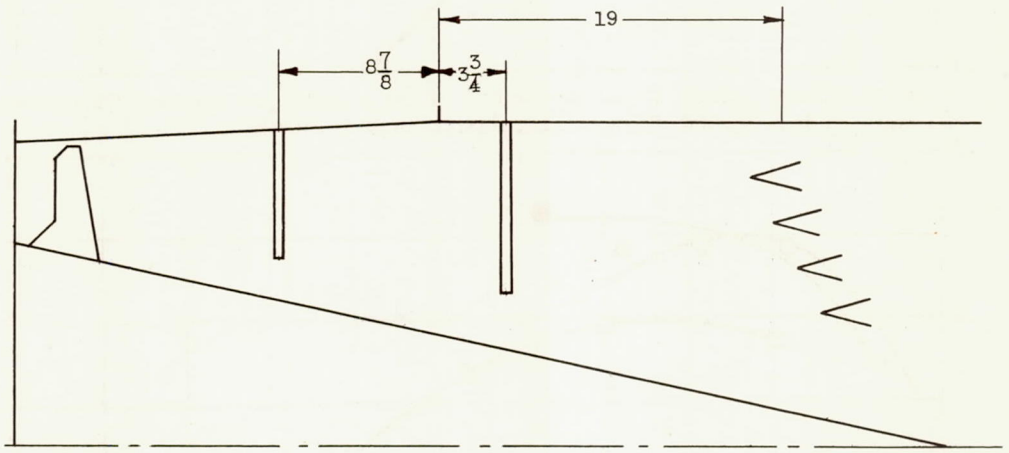

(b) Configuration 7.

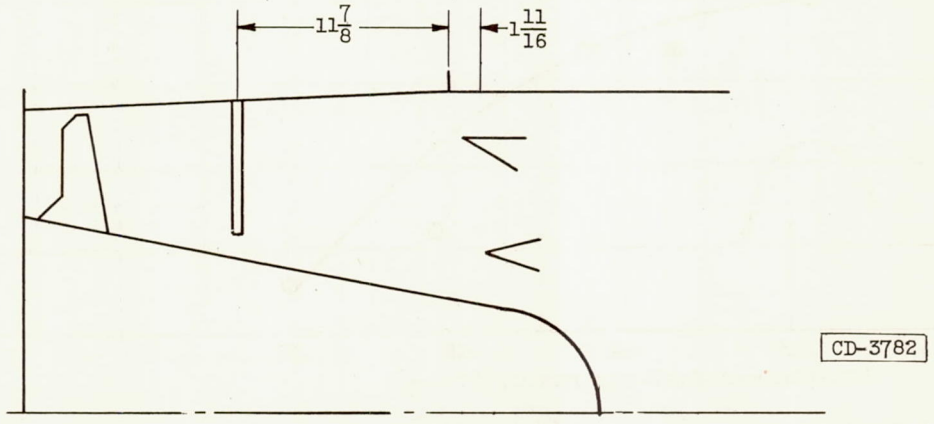

(c) Configuration 8.

Figure 16. - Schematic sketches of configurations 6, 7, and 8. (All dimensions in inches.)

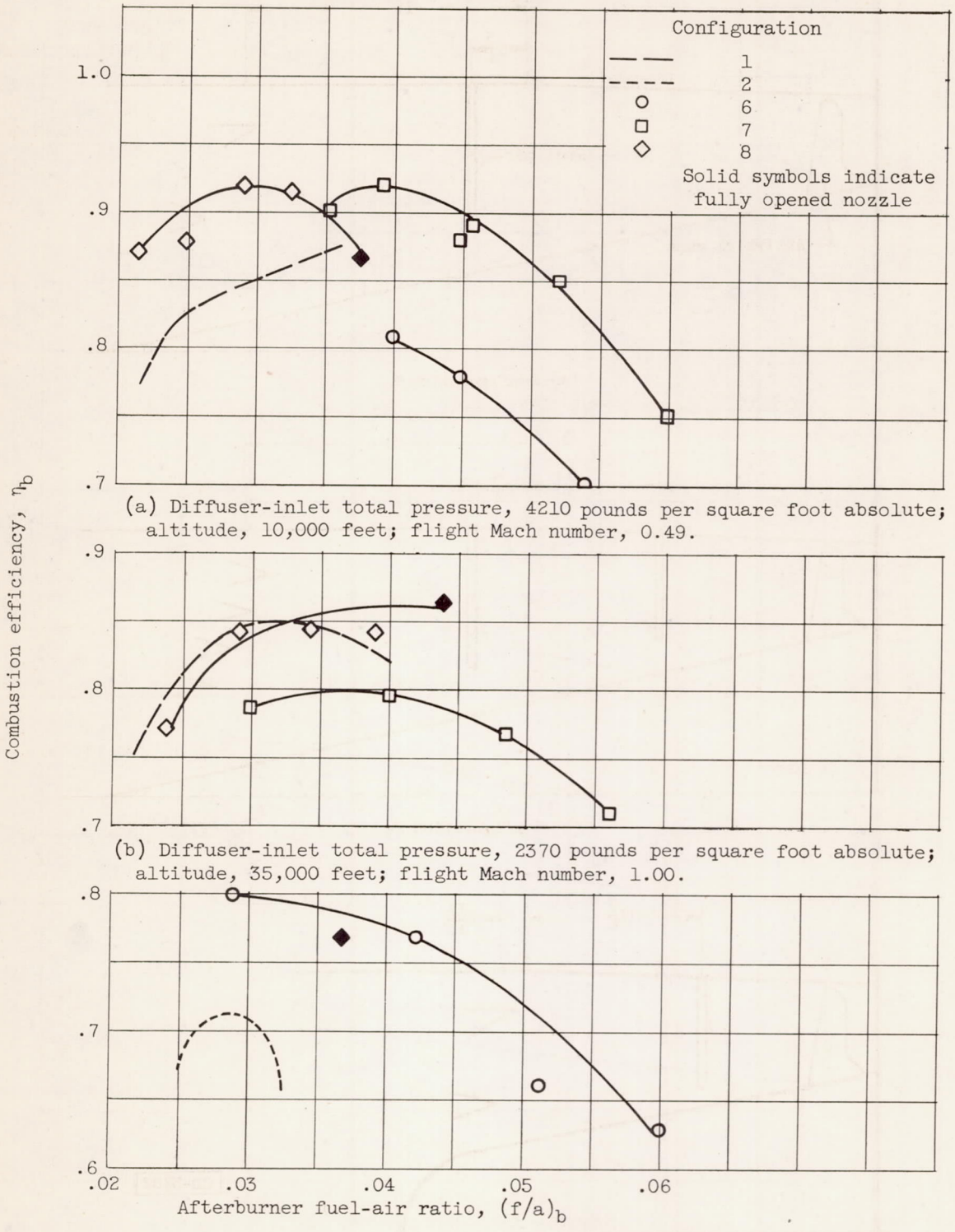

(a) Diffuser-inlet total pressure, 4210 pounds per square foot absolute; altitude, 10,000 feet; flight Mach number, 0.49.

(b) Diffuser-inlet total pressure, 2370 pounds per square foot absolute; altitude, 35,000 feet; flight Mach number, 1.00.

(c) Diffuser-inlet total pressure, 760 pounds per square foot absolute; altitude, 45,000 feet; flight Mach number, 0.15.

Figure 17. - Combustion efficiencies of configurations 6, 7, and 8.

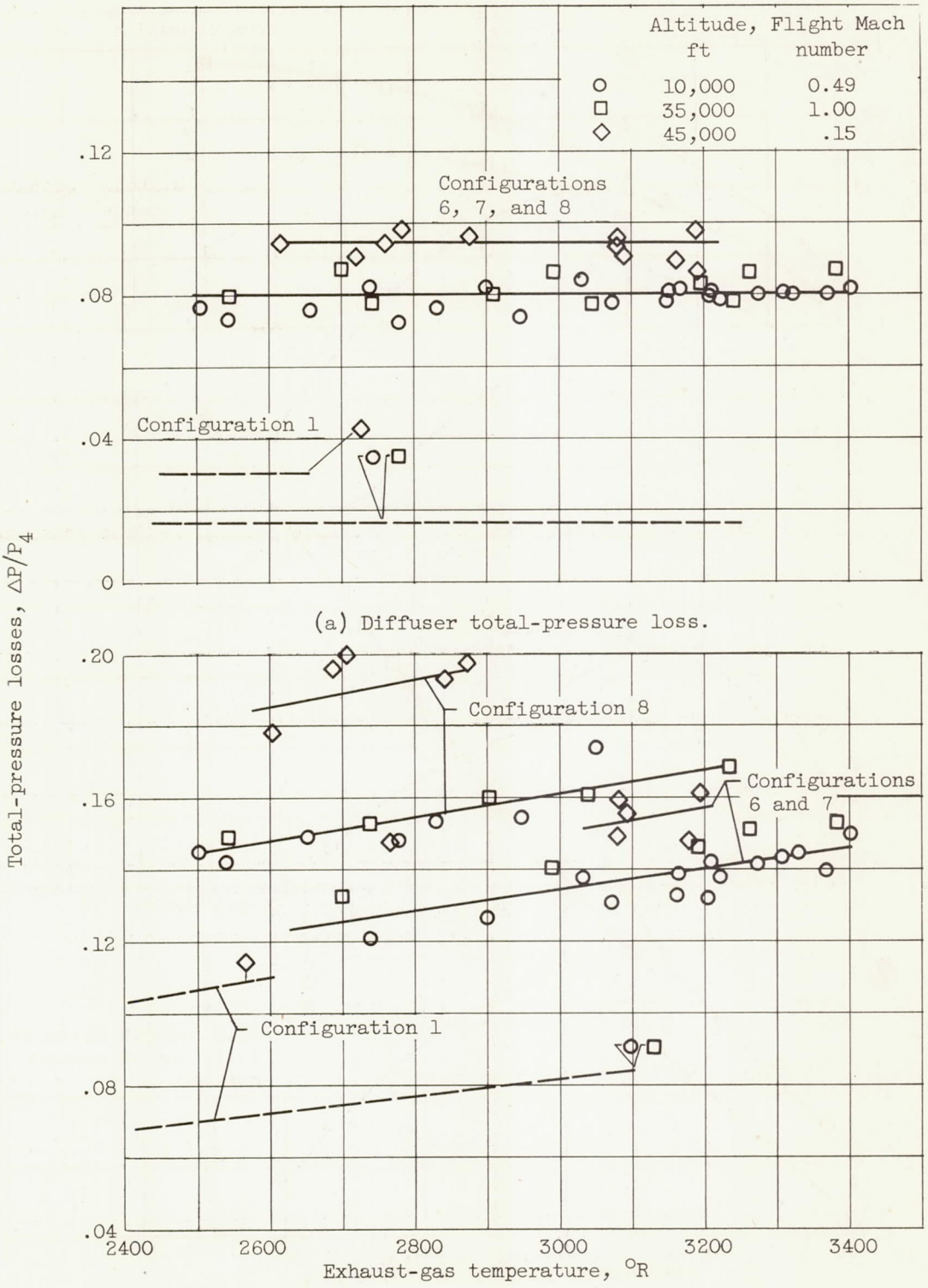

(a) Diffuser total-pressure loss.

(b) Over-all total-pressure loss.

Figure 18. - Total-pressure losses of configurations 6, 7, and 8.

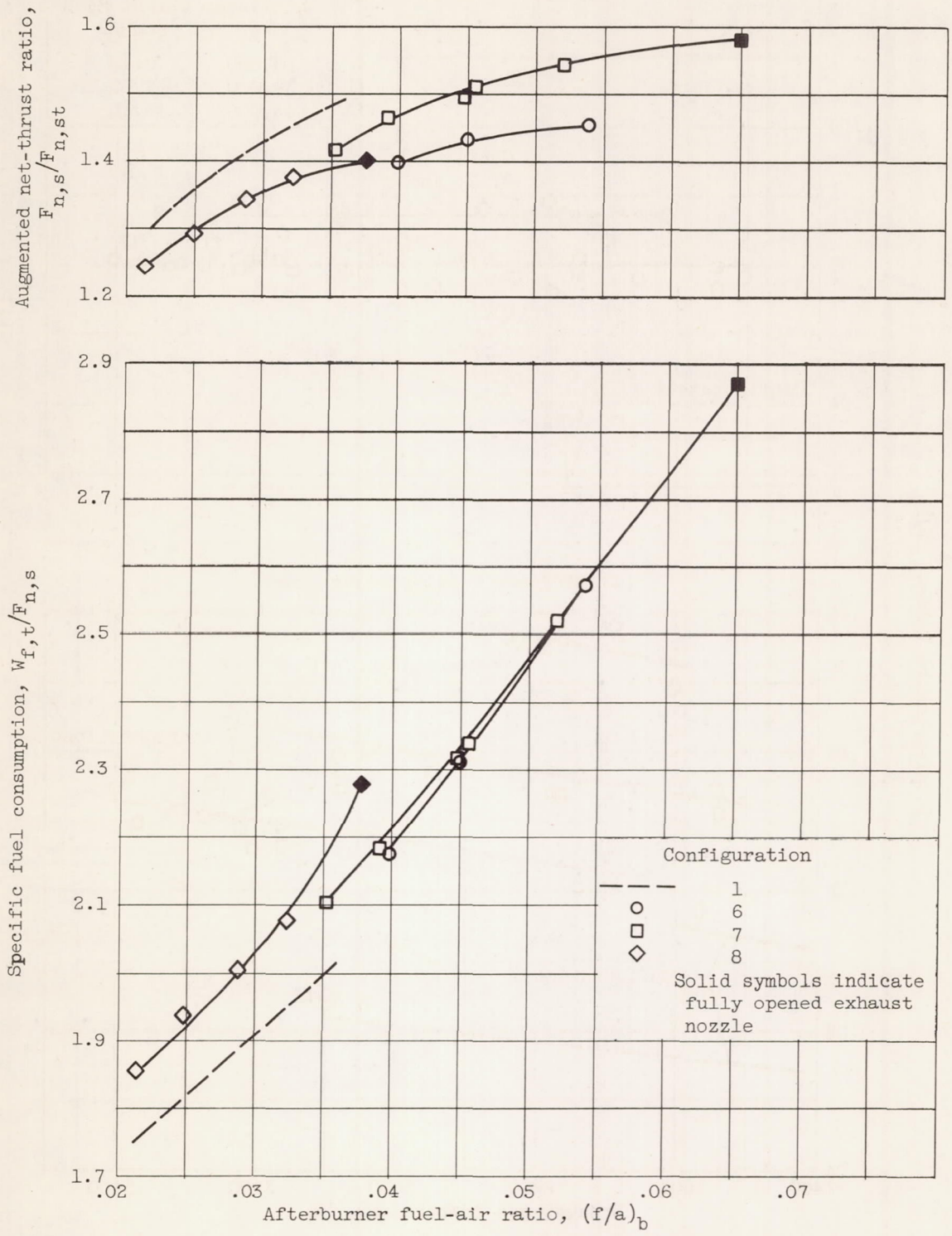

Figure 19. - Afterburner performance of configurations 6, 7, and 8. Altitude, 10,000 feet; flight Mach number, 0.49.

NACA-Langley - 11-17-54 - 325